IAI Journals.ASM.org

Infection with *Francisella tularensis* LVS *clpB* Leads to an Altered yet Protective Immune Response

Lydia M. Barrigan,[a,b] Shraddha Tuladhar,[b] Jason C. Brunton,[a] Matthew D. Woolard,[c] Ching-ju Chen,[d] Divey Saini,[d] Richard Frothingham,[d] Gregory D. Sempowski,[d] Thomas H. Kawula,[a] Jeffrey A. Frelinger[b]

Department of Microbiology and Immunology, University of North Carolina at Chapel Hill, Chapel Hill, North Carolina, USA[a]; Department of Immunobiology, University of Arizona, Tucson, Arizona, USA[b]; Department of Microbiology and Immunology, Louisiana State University Health Sciences Center, Shreveport, Louisiana, USA[c]; Duke Human Vaccine Institute, Durham, North Carolina, USA[d]

Bacterial attenuation is typically thought of as reduced bacterial growth in the presence of constant immune pressure. Infection with *Francisella tularensis* elicits innate and adaptive immune responses. Several *in vivo* screens have identified *F. tularensis* genes necessary for virulence. Many of these mutations render *F. tularensis* defective for intracellular growth. However, some mutations have no impact on intracellular growth, leading us to hypothesize that these *F. tularensis* mutants are attenuated because they induce an altered host immune response. We were particularly interested in the *F. tularensis* LVS (live vaccine strain) *clpB* (FTL_0094) mutant because this strain was attenuated in pneumonic tularemia yet induced a protective immune response. The attenuation of LVS *clpB* was not due to an intracellular growth defect, as LVS *clpB* grew similarly to LVS in primary bone marrow-derived macrophages and a variety of cell lines. We therefore determined whether LVS *clpB* induced an altered immune response compared to that induced by LVS *in vivo*. We found that LVS *clpB* induced proinflammatory cytokine production in the lung early after infection, a process not observed during LVS infection. LVS *clpB* provoked a robust adaptive immune response similar in magnitude to that provoked by LVS but with increased gamma interferon (IFN-γ) and interleukin-17A (IL-17A) production, as measured by mean fluorescence intensity. Altogether, our results indicate that LVS *clpB* is attenuated due to altered host immunity and not an intrinsic growth defect. These results also indicate that disruption of a nonessential gene(s) that is involved in bacterial immune evasion, like *F. tularensis clpB*, can serve as a model for the rational design of attenuated vaccines.

Enormous efforts have gone into detecting bacterial mutations that result in diminished growth *in vivo*. Many of these mutations are the result of a failure of the pathogen to grow *in vitro* and can be attributed to defects in critical aspects of bacterial metabolism. Mutations, for example, that result in auxotrophy render the bacteria incapable of synthesizing essential nutrients such as purines or coenzymes and therefore cause a growth defect. Relatively few mutations that cause bacterial attenuation have been demonstrated to be the result of a failure of the pathogen to interfere with host immune responses. In this article, we focus on one mutation that likely falls into this class of altered host immunity.

Francisella tularensis is a Gram-negative coccobacillus and the causative agent of the zoonotic disease tularemia. Inhalation of as few as 10 virulent type A *F. tularensis* organisms can cause fatal disease in humans (1). This low infectious dose, the ability to persist in the environment, the ease of aerosolization, and the high morbidity and mortality have earned *F. tularensis* a category A select agent classification (2). In fact, *F. tularensis* has been used as the infectious agent in bioweapons and continues to present a real threat today (3, 4). It is therefore critical to understand both infection and pathogenesis. Many attenuating mutations of *Francisella* have been described (5–7), but little information is available on the immune response to attenuated mutants, beyond whether they can protect from secondary challenge with wild-type bacteria.

Experiments utilizing *F. tularensis* as the infectious agent typically use three strains that differ widely for virulence in humans and mice. *F. tularensis* subsp. *tularensis* SchuS4 is a type A strain and must be handled under biosafety level 3 (BSL-3) conditions because of its low infectious dose and its ability to be transmitted via aerosol. SchuS4 is highly pathogenic in mice, with a 100% lethal dose (LD_{100}) of <10 CFU (8). Mice inoculated with SchuS4 succumb to infection within 6 days of inoculation (9), making studies of the adaptive immune response in nonmanipulated mice impossible. For our experiments, we used the type B strain *F. tularensis* subsp. *holarctica* LVS (live vaccine strain). LVS is attenuated in humans and mice compared to SchuS4. Although LVS was widely used in eastern Europe as a vaccine, it is unlikely to ever be licensed in the United States. The intranasal LD_{50} of LVS is approximately 1,000 CFU in mice (8), allowing us to examine aspects of adaptive immunity using an intranasal inoculation dose of 500 CFU. The third strain commonly used is *Francisella novicida* U112, which is avirulent in immunocompetent humans but is highly virulent in mice, with a low infectious dose and rapid death, similar to SchuS4.

The immune response to *F. tularensis* is multilayered and complex, requiring components of both innate and adaptive immunity. The bacterium has evolved several strategies to evade or subvert the host's immune response so that it can persist in the host.

Received 14 February 2013 **Accepted** 13 March 2013
Published ahead of print 25 March 2013
Editor: J. L. Flynn
Address correspondence to Jeffrey A. Frelinger, jfrelin@email.arizona.edu.
Supplemental material for this article may be found at http://dx.doi.org/10.1128/IAI.00207-13.

doi:10.1128/IAI.00207-13

First, *F. tularensis* infects a variety of innate immune cells during infection in the lung, including macrophages, dendritic cells, monocytes, and neutrophils (10, 11). *F. tularensis* also expresses a form of lipopolysaccharide (LPS) that does not efficiently stimulate Toll-like receptor 4 (TLR4) (12). LVS does not stimulate functional maturation (cytokine production) of dendritic cells but does promote phenotypic maturation through the upregulation of CD80 and CD86 (11). SchuS4 does not induce phenotypic or functional maturation of dendritic cells, allowing the bacterium to persist in an immunosuppressed environment (13). Finally, *F. tularensis* lives intracellularly, allowing the bacterium to avoid antibody- and complement-mediated destruction (14).

Because *F. tularensis* replicates within host cells, the T cell response is a critical component for bacterial clearance. Indeed, T cells are required for clearance of *F. tularensis* and the development of protective immunity (15). In particular, gamma interferon (IFN-γ) is required for controlling *F. tularensis* infection. When IFN-γ is blocked by antibody, there is an increase in the bacterial burden, and mice deficient in IFN-γ succumb to an LVS inoculum dose that is sublethal in wild-type mice (16, 17). Administration of recombinant IFN-γ to infected mice decreases bacterial burdens, confirming this cytokine's importance in the control of the infection (18). Th17 cells are also induced in the lung following intranasal inoculation (19). Interleukin-17A (IL-17A)-deficient mice have increased bacterial burdens compared to those in wild-type mice, and administration of IL-17-neutralizing antibody also increased bacterial burdens, highlighting this cytokine's importance during respiratory tularemia (20, 21).

Several *in vivo* screens have identified *F. tularensis* virulence determinants in U112, LVS, and SchuS4 (5–7). A *F. tularensis* mutant could be attenuated if the mutation disrupts expression of a gene necessary for intracellular growth, such as the genes within the pathogenicity island (22). A *F. tularensis* mutant could also be attenuated if the disrupted gene causes the strain to become an auxotroph (5–7). When a mutation does not cause an intracellular growth defect, a strain's attenuation could be the result of a failure to evade the host's immune response. We were interested in characterizing the immune response to an attenuated LVS mutant, LVS *clpB* (FTL_0094). *clpB* encodes a highly conserved chaperone protein of the AAA^+ superfamily of ATPases. *F. tularensis* ClpB is involved in the response to oxidative, ethanol, and acid stresses (23). LVS *clpB* and SchuS4 *clpB* strains are attenuated when delivered by intradermal, intraperitoneal, or oral inoculation routes (23–25). Previous infection with LVS *clpB* and SchuS4 *clpB* provided protection during wild-type challenge (23–25). However, the host's primary immune response to LVS *clpB* that elicits protection during wild-type challenge has not yet been examined.

In this study, we examined the innate and adaptive immune response following intranasal infection with LVS or LVS *clpB*. Our LVS *clpB* strain did not show any defects in intracellular growth in primary bone marrow-derived macrophages (BMDMs) or several cell lines. Because there were no differences in growth, we hypothesized that the attenuation of LVS *clpB* was due to an altered immune response. Indeed, LVS *clpB* induced altered innate and adaptive immune responses compared to those induced by LVS. Other groups have shown that SchuS4 *clpB* and LVS *clpB* are attenuated *in vivo*, but the potential mechanism(s) causing attenuation has not been described (23–25). The work presented here describes the immune response that contributes to the attenuation of LVS *clpB*. The studies also highlight the potential use of *clpB* as a target for attenuation because milder disease is caused while still inducing a robust protective immune response in the lung.

MATERIALS AND METHODS

Bacteria. The live vaccine strain of *Francisella tularensis* subsp. *holarctica* (LVS) was obtained from the CDC (Atlanta, GA). *F. tularensis* subsp. *tularensis* (SchuS4) was obtained from BEI Resources (Manassas, VA). Bacteria were grown on chocolate agar supplemented with 1% IsoVitalex (Becton, Dickinson), brain heart infusion (BHI) broth supplemented with 1% IsoVitalex, or Chamberlain's defined medium (CDM) (26). When necessary, kanamycin (10 μg/ml) or hygromycin (200 μg/ml) was added for antibiotic selection. Bacteria were grown at 37°C. To prepare bacterial inocula, bacteria were removed from a lawn grown on chocolate agar and resuspended in sterile phosphate-buffered saline (PBS) at an optical density at 600 nm (OD_{600}) of 1 (equivalent to 1×10^{10} CFU/ml). Appropriate dilutions were made in sterile PBS to obtain the desired bacterial dose. The number of viable bacteria was quantified by serial dilution and plating onto chocolate agar. The LVS *clpB*::Tn strain was generated by using the EZ-Tn*5* system (Epicentre). The insertion in *clpB* mapped to nucleotide 89763. The LVS *clpB* (FTL_0094) and LVS *dotU* (FTL_0119) deletion strains were generated by using the suicide vector pMP812 (27) containing an amplified region of *clpB* or *dotU*.

Bacterial growth curves. In a 96-well plate, CDM or BHI broth was inoculated with LVS, LVS *clpB*, or LVS *dotU* so that the starting OD_{600} was 0.01. The OD_{600} was measured every 15 min for 48 h by using a Tecan Infinite M200 plate reader capable of maintaining 37°C and 5% CO_2 while shaking.

Mice. C57BL/6J (B6), B6.SJL-*Ptprc*^{a}*Pepc*^{b}/BoyJ (B6-CD45.1), and BALB/cByJ (BALB/c) mice were obtained from The Jackson Laboratory (Bar Harbor, ME). B6.129S7-*Rag1*^{tm1Mom}/J ($Rag^{-/-}$) mice were purchased from The Jackson Laboratory and then bred in-house. All mice were housed under specific-pathogen-free conditions at the University of Arizona or Duke University in accordance with their respective Institutional Animal Care and Use Committees. Female B6 and BALB/c mice used for infections were between 7 and 12 weeks of age.

Cell lines and BMDM generation. J774.1, MH-S, and A549 cells were obtained from the ATCC (Manassas, VA). J774.1 and A549 cells were cultured in Dulbecco's modified Eagle's medium (DMEM) supplemented with 10% fetal bovine serum (Atlas), L-glutamine (HyClone), sodium pyruvate (HyClone), and penicillin-streptomycin (Life). MH-S cells were cultured in RPMI 1640 supplemented with 10% fetal bovine serum (Atlas), L-glutamine (HyClone), sodium pyruvate (HyClone), and penicillin-streptomycin (Life). Medium was replaced with antibiotic-free medium 24 h prior to inoculation with *F. tularensis*. BMDMs were generated from B6 bone marrow as previously described (28).

***In vitro* growth assays.** A total of 1×10^6 cells/well (BMDM, J774, and MH-S) or 0.5×10^6 cells/well (A549) were seeded into a 24-well plate for intracellular growth assays and given 2 h to adhere to the plate. Cells were inoculated at a multiplicity of infection (MOI) of 25:1. Infection was facilitated by centrifugation at $300 \times g$ for 5 min. Cells were inoculated for 2 h with bacteria, and the medium was then removed. Medium containing 50 μg/ml gentamicin (Sigma) was added to kill extracellular bacteria. One hour after gentamicin addition, medium was removed, and the cells were washed twice before the addition of fresh medium. To determine intracellular growth, medium was removed at 4 or 24 h postinfection, and 1 ml of PBS was added to the cells. Cells were removed from the plate by scraping and pipetting vigorously up and down. Cells were lysed by vortexing at maximal speed for 1 min. Serial 1:10 dilutions of the lysate were made and plated onto chocolate agar. The resulting colonies were counted 72 h later.

Inoculation of mice. Mice were anesthetized with 575 mg/kg of body weight of tribromomethanol (Avertin; Sigma) administered intraperitoneally. Mice were then intranasally inoculated with 5×10^2 CFU LVS, 5×10^4 CFU LVS *clpB*, or 5×10^5 CFU LVS *dotU* suspended in 50 μl PBS. For

high-dose LVS challenge experiments, mice were anesthetized with 0.25 ml of a cocktail of 7.5 mg/ml ketamine and 0.5 mg/ml xylazine in PBS. Mice were then intranasally inoculated with 5×10^3 CFU LVS. For SchuS4 challenge, approximately 30 CFU of SchuS4 were administered via the aerosol route in a BSL-3 chamber. Mice were weighed daily following all inoculations. Mice were sacrificed if they lost more than 25% of their starting weight, as indicated in the University of Arizona and Duke IACUC protocols.

Determination of bacterial burdens. Spleens, livers, and lungs were homogenized in sterile PBS by using a Biojector (Bioject). Tenfold serial dilutions were made and plated onto chocolate agar. The resulting colonies were counted 72 h later. The limit of detection was 50 CFU per organ.

Collection of bronchoalveolar lavage fluid. Mice were sacrificed, and the trachea was exposed. A 22-gauge catheter was inserted into the trachea and secured with a suture. The lungs were fully inflated with 800 μl of PBS and washed three times. Cells were removed from the bronchoalveolar lavage fluid (BALF) by centrifugation. Collected lavage fluid was frozen at −80°C until Luminex analysis was performed.

Depletion of IFN-γ. Purified XMG1.2 (anti-IFN-γ) antibody was a generous gift from Mary Ann Accavitti-Loper at the SERCEB Mouse Monoclonal Antibody Core (University of Alabama—Birmingham). Rat IgG1 isotype control antibody (anti-HRPN) was purchased from BioXCell (West Lebanon, NH). Mice were administered 500 μg of depleting or control antibody in 200 μl PBS via intraperitoneal injection on days 0 and 2 postinoculation.

Luminex analysis. A multiplex Luminex bead-based approach was used to quantify cytokines/chemokines in BALF or clarified tissue homogenate. A 20-analyte assay panel was performed according to the manufacturer's protocol (Invitrogen), using a BioPlex array reader (Bio-Rad Laboratories). Using integrated cytokine/chemokine standard curves, the assay reports the following analytes in pg/ml: fibroblast growth factor (FGF) basic, granulocyte-macrophage colony-stimulating factor (GM-CSF), IFN-γ, IL-1α, IL-1β, IL-2, IL-4, IL-5, IL-6, IL-10, IL-12 (p40/p70), IL-13, IL-17, KC, monocyte chemoattractant protein 1 (MCP-1), monokine induced by IFN-γ (MIG), macrophage inflammatory protein 1α (MIP-1α), tumor necrosis factor alpha (TNF-α), and vascular endothelial growth factor. A five-parameter nonlinear logistic regression model was used to a establish standard curve and to estimate the probability of occurrence of a concentration at a given point. Standard outliers were removed from the analysis if the observed/expected percent recovery was outside the acceptable limits (70 to 130%). Upper and lower levels of quantification were determined by use of BioPlex Manager software based on goodness of fit and percent recovery. Calculated pg/ml for experimental specimens were multiplied by the inherent assay dilution factor (df = 2) and reported as final observed pg/ml.

Collection of spleen and lung cells. Spleens were harvested from mice and made into a single-cell suspension. Red blood cells were lysed by using ammonium chloride-potassium carbonate lysis buffer. Lungs were perfused with PBS to remove blood and then finely minced. Minced lung was placed into 10 ml of digestion buffer containing 0.5 mg/ml collagenase I (Worthington Biochemical), 0.02 mg/ml DNase (Sigma), and 125 U/ml elastase (Worthington Biochemical) in RPMI 1640 (HyClone). Lungs were digested for 30 min at 37°C and then vigorously pipetted prior to filtering through a 100-μm filter. Mononuclear cells were isolated from the single-cell suspension by density gradient centrifugation over Lympholyte M (Cedarlane Labs). Viable cells from spleen and lung were determined by trypan blue exclusion using a hemacytometer.

Antibodies. The following directly conjugated antibodies were utilized for flow cytometry analysis: CD3 Alexa Fluor 488 (AF488) (clone 145-2C11; eBioscience), CD4 AF700 (clone GK1.5; Biolegend), CD8a V500 (clone 53-6.7; BD Biosciences), CD45.1 phycoerythrin (PE)-Cy7 (clone A20; Biolegend), T cell receptor (TCR) γδ peridinin chlorophyll protein (PerCP)-Cy5.5 (clone GL3; Biolegend), IFN-γ PE (clone XMG1.2; BD Biosciences), IL-17A AF647 (clone TC11-18H10.1; Biolegend), CD11b Pacific Blue (clone M1/70; Biolegend), CD11c Pacific Blue (clone N418; Biolegend), CD19 Pacific Blue (clone 6D5; Biolegend), F4/80 Pacific Blue (clone BM8; Biolegend), GR-1 (Ly-6G) eFluor 450 (clone RB6-8C5; eBioscience), and NK1.1 Pacific Blue (clone PK136; Biolegend). All antibodies were titrated on normal B6 splenocytes prior to use.

Intracellular cytokine staining. Splenocytes from B6-CD45.1 cells were used as antigen-presenting cells. B6-CD45.1 cells were added at 2×10^6 cells/well in a 24-well plate or at 0.5×10^6 cells/well in a 48-well plate and infected with LVS at an MOI of 200:1 or mock infected. At 2 h postinfection, the medium was removed, and 5 μg/ml gentamicin was added to kill any extracellular bacteria. Splenocytes were cultured overnight in the presence of gentamicin. Prior to coculture with cells isolated from infected mice, antigen-presenting cells were washed extensively to remove any cytokine or prostaglandin E_2 (PGE_2) that could interfere with the coculture. Cells isolated from mice were cocultured at a 1:1 ratio with infected or mock-infected splenocytes for 24 h. During the last 4 h of culture, 10 μg/ml brefeldin A (Sigma) was added to each well to stop cytokine secretion. Cells were removed from the plate and stained with Pacific Blue succimidyl ester (Invitrogen) to distinguish live and dead cells. Cells were then stained with antibodies for surface markers. Following fixation and permeabilization of the cells, cells were stained for IFN-γ and IL-17A. Cells were washed extensively after each staining step to remove residual unbound antibody.

Gating strategy for T cell analysis. The gating scheme is shown in Fig. S1 in the supplemental material. Single cells were discriminated from doublets by plotting linear side scatter versus side-scatter area. Cells were then selected by plotting side-scatter area versus forward-scatter area. Live $CD3^+$ T cells were then selected by plotting CD3 versus the Pacific Blue channel, which included the live/dead stain and markers for antigen-presenting cells. From the $CD3^+$ gate, $CD4^+$ and $CD8^+$ T cells were selected. Gates for IFN-γ- and IL-17A-positive cells were set based on isotype control staining. Delta mean fluorescent intensity (ΔMFI) for each sample was determined by subtracting the cytokine-negative population from the cytokine-positive population. FlowJo v7.6 (Treestar) was used for all flow cytometry analyses.

Determination of IFN-γ and IL-17A secretion by purified $CD4^+$ T cells. B6 splenocytes were depleted of T cells by using mouse Thy1.2 Dynabeads (Life Technologies) and used as antigen-presenting cells. A total of 5×10^4 T cell-depleted splenocytes/well were seeded into a 96-well plate and then infected with LVS at an MOI of 200:1 or mock infected. At 2 h postinfection, the medium was removed, and 5 μg/ml gentamicin was added to kill any extracellular bacteria. T cell-depleted splenocytes were cultured overnight in the presence of gentamicin. Prior to coculture with purified $CD4^+$ T cells from infected mice, antigen-presenting cells were washed extensively to remove any cytokine or PGE_2 that could interfere with the coculture. $CD4^+$ T cells were enriched from single-cell suspensions of lung cells or splenocytes by using a Dynabeads Untouched Mouse CD4 Cells kit (Life Technologies). Enriched $CD4^+$ T cells were cocultured at a 1:1 ratio with T cell-depleted LVS-infected or mock-infected splenocytes for 24 h. Culture supernatant was then removed and stored at −20°C until enzyme-linked immunosorbent assay (ELISA) analysis was performed. Each sample was tested in triplicate. The IFN-γ concentration was determined by using a mouse IFN-γ Instant ELISA (eBioscience), and the IL-17A concentration was determined by using a mouse IL-17A Ready-Set-Go ELISA (eBioscience). T cell depletion and $CD4^+$ T cell enrichment were determined by flow cytometry analysis. IFN-γ and IL-17A concentrations were normalized based on the number of $CD4^+$ T cells in the culture, as determined by flow cytometry.

Statistical analysis. Data were analyzed by using a one-way analysis of variance (ANOVA) with Tukey's posttest for cytokine levels and flow cytometry results. Bacterial burdens were log transformed, and Student's *t* test or ANOVA with Tukey's posttest was then applied. For LVS protection studies, a chi-square test with Yates' correction was applied. GraphPad Prism (v5.04) was used for analysis. Error bars show standard errors of the means. Significance levels are indicated in the figures as follows: *

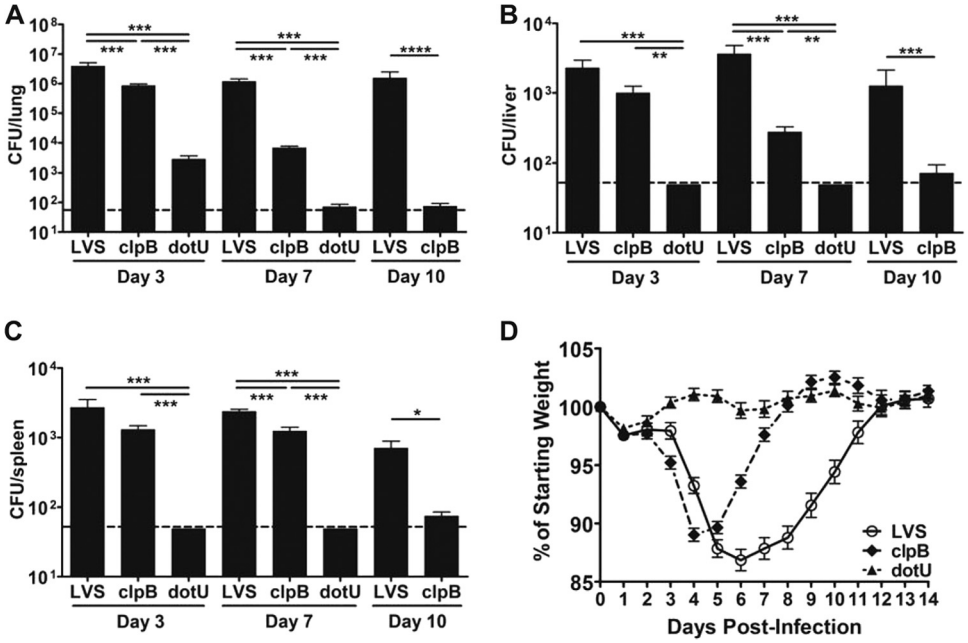

FIG 1 LVS *clpB*-infected mice clear bacteria faster and exhibit less disease. B6 mice were intranasally inoculated with LVS (5×10^2 CFU), LVS *clpB* (5×10^4 CFU), or LVS *dotU* (5×10^5 CFU). (A to C) On days 3, 7, and 10 postinoculation, bacterial burdens in the lung (A), liver (B), and spleen (C) were determined by plating serial dilutions of organ homogenate onto chocolate agar ($n = 5$ to 12 mice/group). Data are combined from at least 4 independent experiments per time point. The dashed line indicates the limit of detection of 50 CFU. Statistical significance was determined on log-transformed data by using ANOVA with Tukey's posttest (days 3 and 7) or Student's *t* test (day 10). (D) Mouse weight was determined daily and is reported as a percentage of the starting weight ($n = 25$ to 32 mice/group).

indicates a *P* value of <0.05, ** indicates a *P* value of <0.01, *** indicates a *P* value of <0.001, and **** indicates a *P* value of <0.0001.

RESULTS

LVS *clpB* is attenuated in mouse pneumonic tularemia. Several groups have shown that LVS *clpB* or SchuS4 *clpB* strains are attenuated following either intradermal, intraperitoneal, or oral inoculation in either BALB/c or C3H/HeN mice (23–25). We were interested in determining whether LVS *clpB* was also attenuated in a pneumonic tularemia model in C57BL/6J (B6) mice. For this study, we produced two LVS *clpB* mutant strains. One strain carried a transposon (Tn) insertion in the *clpB* gene, and the other was an in-frame deletion of the *clpB* coding sequence. The mutations were confirmed by DNA sequencing. Although transposon mutations can have polar effects, we did not expect any from the transposon insertion in *clpB* because bioinformatic analysis indicated that *clpB* is not located in an operon (23). Indeed, we found that the *clpB*::Tn mutant and the deletion strain behaved identically in all experiments. We have therefore combined all data and simply refer to infection with either strain as LVS *clpB*.

Initial experiments demonstrated that LVS *clpB* did not disseminate when an inoculation dose of 500 CFU was used, despite this dose causing disease following LVS inoculation. We therefore conducted preliminary experiments to establish the dose of LVS *clpB* that produced a similar peak bacteremia in the spleen so that mice were exposed to similar antigen levels. Similar antigen loads are important because in other infection models, the magnitude of the primary adaptive immune response was influenced by the peak bacterial load and not the duration of infection (29–31). As a control for inoculation with a bacterial strain that failed to grow intracellularly, we selected LVS *dotU* (32). We achieved similar burdens for LVS and LVS *clpB*, but since LVS *dotU* fails to grow intracellularly (32), this strain was inoculated at the highest practical dose. Seven- to twelve-week-old B6 mice were intranasally inoculated with 5×10^2 CFU LVS, 5×10^4 CFU LVS *clpB*, or 5×10^5 CFU LVS *dotU*. To determine bacterial growth *in vivo*, mice were euthanized on days 3, 7, and 10 postinoculation, and bacterial burdens in the spleen, liver, and lung were determined by plating serial dilutions of tissue homogenate onto chocolate agar (Fig. 1A to C). While LVS *clpB* and LVS bacterial burdens were not significantly different in the spleen and liver at 3 days postinoculation, LVS *clpB* bacteria were cleared much faster than LVS from all organs tested. Few LVS *clpB* colonies were recovered at 10 days postinoculation, while LVS-infected mice still had high bacterial loads, particularly in the lung. Despite the 1,000-fold-higher dose of LVS *dotU* than of LVS, the number of colonies recovered from the lungs at 3 days postinoculation was 1,000-fold lower than the number of LVS colonies. Viable LVS *dotU* organisms were recovered from isolated lung cells from LVS *dotU*-infected mice harvested at 3 days postinoculation and cultured in gentamicin for 1 h, demonstrating that LVS *dotU* was internalized and that the bacteria had not simply persisted in the extracellular space (see Fig. S2 in the supplemental material). Despite its intracellular location, LVS *dotU* failed to leave the lung and transit to the spleen and liver and was effectively cleared by 7 days postinoculation in all organs tested. Because LVS *dotU* was not found in distal organs on day 3 postinoculation, but infected cells were still present in the lung, these data suggest that infected cells were not the primary method of dissemination. Alternatively, the LVS *dotU*-infected cells were not activated in a manner that caused them to leave the primary site of infection. To confirm that rapid clearance of LVS

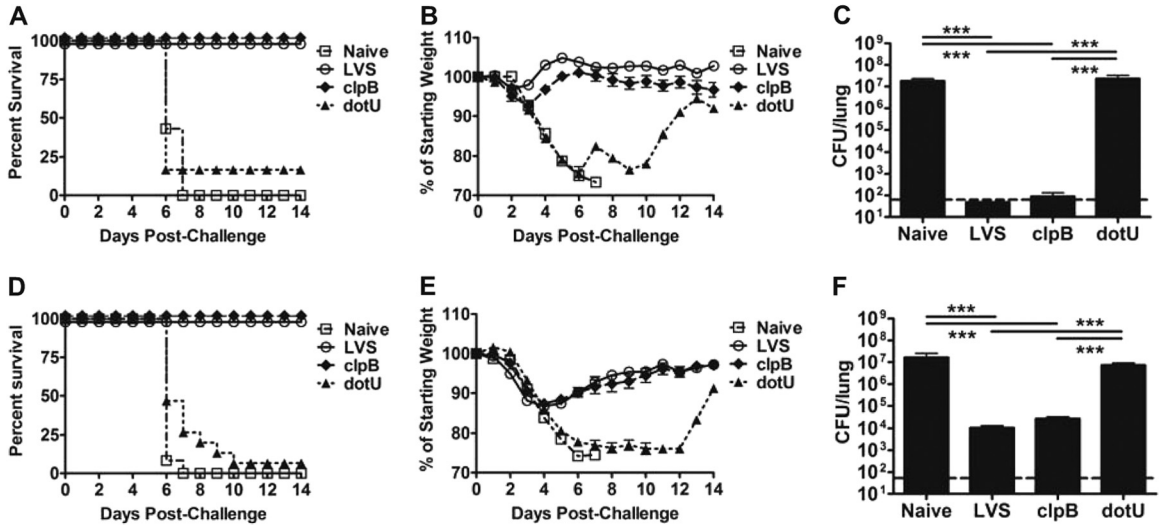

FIG 2 LVS *clpB* protects against a lethal secondary LVS challenge 28 or 120 days after primary infection. B6 mice were intranasally inoculated with LVS (5×10^2 CFU), LVS *clpB* (5×10^4 CFU), or LVS *dotU* (5×10^5 CFU) or left uninfected. (A) Twenty-eight days after primary infection, mice were challenged intranasally with 5×10^3 CFU LVS, and survival was measured ($n = 6$ to 12 mice/group). Data are combined from 2 independent experiments. A chi-square test with Yates' correction was used to compare survival of the vaccinated groups to that of the naïve group (naïve versus LVS, $P \leq 0.001$; naïve versus LVS *clpB*, $P \leq 0.0001$; naïve versus LVS *dotU*, not significant). (B) Mice were weighed daily following secondary infection with LVS, and weight loss is reported as a percentage of the starting weight. Weight loss by the surviving LVS *dotU*-vaccinated mouse is reported ($n = 6$ to 12 mice/group). Data are combined from 2 independent experiments. (C) Bacterial burdens in the lung on day 6 after rechallenge ($n = 5$ to 7 mice/group). Data are compiled from 2 independent experiments. The dashed line indicates the limit of detection of 50 CFU. Statistical significance was determined on log-transformed data by using ANOVA with Tukey's posttest. (D) One hundred twenty days after primary infection, mice were challenged with 5×10^3 CFU LVS, and survival was measured ($n = 12$ to 15 mice/group). Data are combined from 2 independent experiments. A chi-square test with Yates' correction was used to compare survival of the vaccinated groups to the naïve group (naïve versus LVS, $P \leq 0.001$; naïve versus LVS *clpB*, $P \leq 0.0001$; naïve versus LVS *dotU*, not significant). (E) Mice were weighed daily following secondary infection with LVS, and weight loss is reported as a percentage of the starting weight. Weight loss by the surviving LVS *dotU*-vaccinated mouse is reported ($n = 12$ to 15 mice/group). Data are combined from 2 independent experiments. (F) Bacterial burdens in the lung on day 6 after rechallenge ($n = 6$ to 8 mice/group). Data are combined from 2 independent experiments. The dashed line indicates the limit of detection of 50 CFU. Statistical significance was determined on log-transformed data by using ANOVA with Tukey's posttest.

clpB and LVS *dotU* was due specifically to the absence of these genes, the strains were *trans*-complemented. B6 mice were intranasally inoculated with 5×10^2 CFU of LVS *clpB* complement or LVS *dotU* complement. We used the same dose as LVS since transcomplementation should return these strains to wild-type LVS virulence levels. Indeed, transcomplementation of LVS *clpB* and LVS *dotU* led to bacterial burdens comparable to those of LVS in the spleen, liver, and lungs at 3 days postinoculation (see Fig. S3 in the supplemental material). Overall, these results demonstrate that LVS *clpB* is attenuated in a pneumonic model of tularemia, just as other groups have shown for LVS *clpB* and SchuS4 *clpB* by different routes of inoculation (23–25).

We also wanted to understand if the extent of disease caused by LVS *clpB* was similar to that caused by LVS. As a measure of overall health, body weight change is a reasonable measure of clinical status. Infected mice were weighed daily, and weight loss as a percentage of the starting weight was reported (Fig. 1D). LVS-infected mice lost nearly 15% of their starting weight by day 7 and then slowly regained weight. In contrast to LVS, LVS *clpB*-infected mice only lost approximately 10% of their starting weight and began to regain weight at 5 days postinoculation. LVS *clpB*-infected mice regained their lost weight more rapidly than did LVS-infected mice, which correlated with faster bacterial clearance. Mice infected with LVS *dotU* did not lose any weight, an expected result given that the bacteria failed to grow *in vivo*. Together, these results indicate that LVS *clpB* is attenuated in pneumonic tularemia and leads to a weight loss profile that differed from that of LVS infection.

Previous infection with LVS *clpB* protects against lethal LVS intranasal challenge. We next sought to determine whether previous intranasal inoculation with LVS, LVS *clpB*, or LVS *dotU* elicits an immune response that was protective against a subsequent lethal LVS intranasal challenge. Mice were intranasally inoculated with 5×10^2 CFU LVS, 5×10^4 CFU LVS *clpB*, or 5×10^5 CFU LVS *dotU*. To examine the early memory response, mice were challenged with 5×10^3 CFU (approximately 5 LD_{50} [8]) of LVS intranasally 28 days after the initial infection. All mice vaccinated with LVS or LVS *clpB* survived lethal LVS challenge (Fig. 2A). LVS- and LVS *clpB*-vaccinated mice lost little weight following lethal LVS challenge and quickly returned to their starting weight (Fig. 2B). Naïve and LVS *dotU*-vaccinated mice continued to lose weight after LVS- and LVS *clpB*-vaccinated mice began their recovery. The abrupt change in the weight loss curve for the LVS *dotU*-vaccinated group is due to the one surviving mouse. Naïve mice fell below the weight loss threshold at 6 or 7 days after rechallenge. Five of six LVS *dotU*-vaccinated mice succumbed to infection 6 days after the lethal dose challenge. There was no significant difference in survival when LVS *dotU*-vaccinated mice were compared to the naïve group. The surviving LVS *dotU*-vaccinated mouse lost more than 20% of its starting weight but never fell below the 25% threshold after challenge with LVS. Despite sustained illness, indicated by weight loss in this mouse, there were no colonies recovered from the spleen, liver, or lung 14 days following the lethal challenge, similar to mice following primary exposure to LVS.

When naïve and LVS *dotU*-vaccinated mice were sacrificed upon losing >25% of their starting weight (day 6 after rechallenge), we harvested spleen, liver, and lung and determined bacterial burdens (Fig. 2C). We also harvested spleen, liver, and lung from LVS- and LVS *clpB*-vaccinated mice on day 6 postinfection and determined bacterial burdens for comparison purposes (Fig. 2C). Naïve and LVS *dotU*-vaccinated mice had high bacterial burdens in the lung, with means exceeding 10^7 CFU. High bacterial burdens were also observed for the spleens and livers of naïve and LVS *dotU*-vaccinated mice compared to the few or no colonies recovered from LVS- or LVS *clpB*-vaccinated mice (data not shown). No colonies were recovered from the lungs of LVS-vaccinated mice and 4 of 6 LVS *clpB*-vaccinated mice.

We were also interested in whether LVS *clpB* would confer long-lived protection against lethal LVS challenge. Mice were intranasally inoculated with 5×10^2 CFU LVS, 5×10^4 CFU LVS *clpB*, or 5×10^5 CFU LVS *dotU* and then challenged with 5×10^3 CFU LVS intranasally 120 days after the initial infection. All LVS- and LVS *clpB*-vaccinated mice survived lethal LVS challenge (Fig. 2D). All naïve mice succumbed to their infection by day 7. Over half of the LVS *dotU*-vaccinated mice succumbed to their infection by day 7, and all but one mouse succumbed by day 14. The surviving LVS *dotU*-vaccinated mouse lost more than 20% of its starting weight but never fell below the 25% threshold for sacrifice. This mouse was sacrificed on day 14, and the bacterial burdens in the spleen, liver, and lung were determined. A total of 125 CFU were recovered from the spleen, 0 CFU were recovered for the liver, and 425 CFU were recovered from the lung, indicating that this mouse was clearing the high-dose LVS challenge. When mice were challenged 120 days after vaccination, the LVS- and LVS *clpB*-vaccinated groups lost more weight (approximately 10 to 15% of their starting weight) than the same groups challenged 28 days after vaccination (Fig. 2E). LVS- and LVS *clpB*-vaccinated mice not only showed equivalent weight loss after high-dose LVS challenge but also regained their lost weight at a similar pace. Naïve and LVS *dotU*-vaccinated mice also showed similar weight loss profiles compared to each other. Figure 2E also shows that the surviving LVS *dotU*-vaccinated mouse exhibited extreme weight loss but rapidly gained weight on days 13 and 14.

When naïve and LVS *dotU*-vaccinated mice fell below the weight loss threshold on day 6, four mice per group were sacrificed, and bacterial burdens in the spleen, liver, and lung were determined (Fig. 2F). Only the number of CFU in the lung is shown; however, a similar trend was seen for the spleen and liver (data not shown). Naïve and LVS *dotU*-vaccinated mice had high bacterial burdens that were comparable to the burdens found when mice were challenged 28 days after vaccination. LVS- and LVS *clpB*-vaccinated mice had approximately 10^4 CFU in their lungs on day 6 after the high-dose LVS challenge. These results clearly indicate that LVS *clpB* protects against subsequent lethal LVS challenge.

Since LVS *clpB* induced a robust adaptive immune response that protected against a lethal LVS challenge, we next wanted to determine whether LVS *clpB* could protect against aerosolized, highly virulent SchuS4. Mice were intranasally inoculated with 5×10^2 CFU LVS, 5×10^4 CFU LVS *clpB*, or 5×10^5 CFU LVS *dotU* and then challenged with 30 CFU SchuS4 (measured as the dose retained in the lungs at 1 h, approximately 30 LD_{100} [8]) via the aerosol route 28 days after the initial infection. The use of aerosolized SchuS4 in B6 mice is a very stringent test of whether LVS *clpB* infection confers protection. Previous vaccination with LVS protected 2 of 7 mice, and LVS *clpB* vaccination protected 1 of 8. These results are consistent with the findings of others who have also shown that previous LVS infection does not fully protect against SchuS4 challenge in B6 mice (33, 34). Naïve and LVS *dotU*-vaccinated mice succumbed to SchuS4 infection at 5 days postinfection. While neither LVS nor LVS *clpB* vaccination provided complete protection against subsequent SchuS4 infection, these infections significantly increased the median survival time from 5 days (naïve) to 9 days (LVS *clpB*) or 10 days (LVS) (see Fig. S4 in the supplemental material). A Mantel-Cox log-rank test was used to compare the survival of the vaccinated groups to the survival of the naïve group. Survival with LVS *dotU* vaccination was not statistically different from that of the naïve group, but LVS and LVS *clpB* vaccination significantly increased survival after SchuS4 challenge ($P \leq 0.001$).

LVS *clpB* does not exhibit an intracellular growth defect. A bacterial strain's attenuation could be the result of a growth defect or an altered immune response that is more effective at bacterial clearance. We therefore sought to determine whether our LVS *clpB* or LVS *dotU* strain had a growth defect in broth or intracellularly that could explain its attenuation *in vivo*. We initially examined the ability of LVS, LVS *clpB*, and LVS *dotU* to grow in either CDM (minimal) or BHI broth (rich). We inoculated cultures with log-phase bacteria and monitored the OD_{600} every 15 min for 48 h. The growth rates of the three strains in CDM and BHI broth were nearly identical (Fig. 3A and B). Therefore, there is no inherent growth difference *in vitro*.

We next determined whether LVS *clpB* or LVS *dotU* had an intracellular growth defect in primary BMDMs or the cell lines A549 (human alveolar type II epithelial), J774 (mouse macrophage), and MH-S (mouse alveolar macrophage). Cells were inoculated with LVS or LVS *clpB* at an MOI of 25:1 for 120 min to allow internalization. Cells were then treated with gentamicin to kill extracellular bacteria. To determine bacterial internalization, macrophages were lysed 4 h after inoculation, and serial dilutions of the lysate were plated onto chocolate agar. We recovered similar numbers of both LVS and LVS *clpB* CFU within each different cell type at 4 h postinoculation, indicating that LVS *clpB* is not defective for internalization (Fig. 3C to F). To determine the ability of LVS *clpB* to grow in BMDMs, we lysed infected cells at 24 h postinoculation and plated serial dilutions of the lysate onto chocolate agar. We found a similar increase in the number of CFU recovered for LVS and LVS *clpB* within each cell line, indicating that LVS *clpB* has no intracellular growth defect (Fig. 3C to F). Because LVS *clpB* grows in a variety of cell lines, these data indicate that the ability of LVS *clpB* to grow intracellularly is generalizable and not specific to a certain cell type. Although LVS *dotU* infected all cells tested so that it was protected from gentamicin similarly to LVS at 4 h postinoculation, this strain failed to grow, and a similar number of or even fewer CFU were recovered at 24 h postinoculation (Fig. 3C to F). We could rescue the intracellular growth defect seen with LVS *dotU* by *trans*-complementation (see Fig. S5 in the supplemental material). These results indicate that the *in vivo* attenuation of LVS *dotU* is likely a consequence of this strain's inability to grow intracellularly. Indeed, LVS *dotU* and U112 *dotU* failed to escape the phagosome (32, 35) to reach the cytosol, the replicative niche of *Francisella*. However, since LVS *clpB* has no intracellular growth defect, its attenuation may be caused by an altered immune response that is more effective at bacterial clearance.

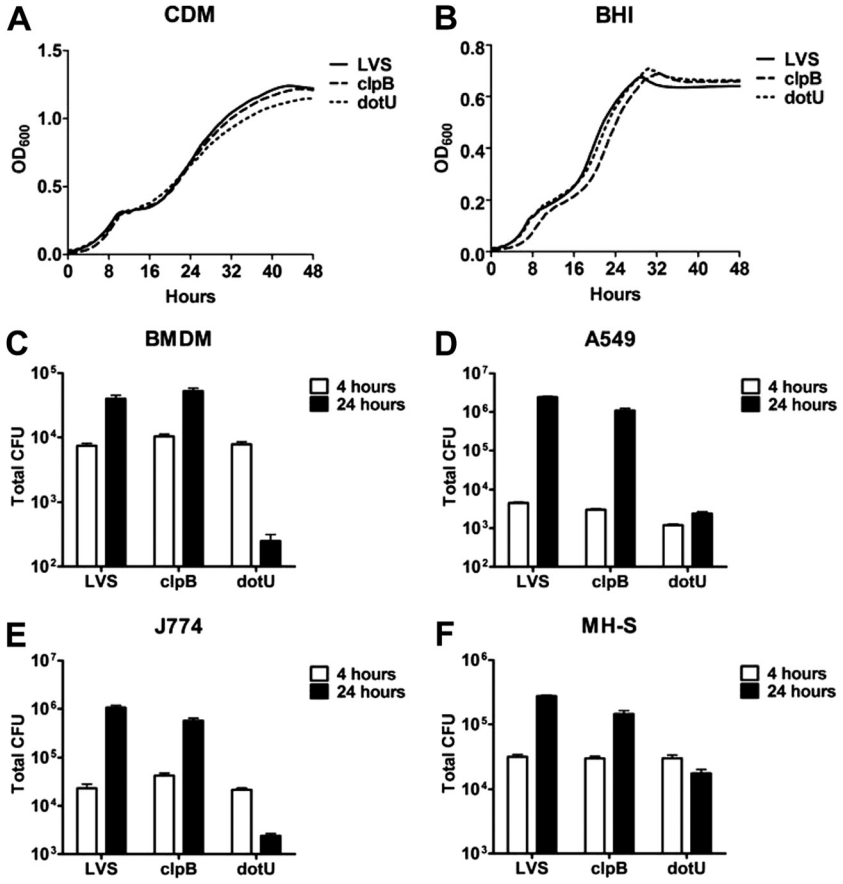

FIG 3 LVS *clpB* does not exhibit an intracellular growth defect. (A and B) LVS, LVS *clpB*, and LVS *dotU* growth in CDM (A) or BHI broth (B) was determined by using a Tecan Infinite M200 plate reader by measuring the OD_{600} every 15 min for 48 h. Data shown are the averages of data from triplicate wells and are representative of at least 3 independent experiments per strain. (C to F) B6 bone marrow-derived macrophages (BMDMs) (C) or A549 (D), J774 (E), or MH-S (F) cells were infected with LVS, LVS *clpB*, or LVS *dotU* at an MOI of 25:1. Cells were lysed at either 4 or 24 h postinoculation, and serial dilutions of the lysate were plated onto chocolate agar to determine the number of bacteria present. Cells were infected with each strain in triplicate, and lysates from each sample were plated in duplicate. Data are representative of at least 2 independent experiments.

LVS *clpB* fails to inhibit early proinflammatory cytokine production in the lung. Because LVS *clpB* did not exhibit an intracellular growth defect, we hypothesized that this strain's attenuation was due to an altered immune response that was more effective at bacterial clearance. To test our hypothesis, we first examined cytokine production in the lung BALF on day 3 postinoculation using a 20-plex mouse cytokine Luminex assay. Despite higher lung bacterial burdens in LVS-infected B6 mice on day 3 postinoculation than in LVS *clpB*-infected B6 mice (Fig. 1A), the BALF of LVS-infected B6 mice contained fewer proinflammatory cytokines and chemokines than the BALF of LVS *clpB*-infected B6 mice (Fig. 4). LVS *clpB* also induced a similar profile of proinflam-

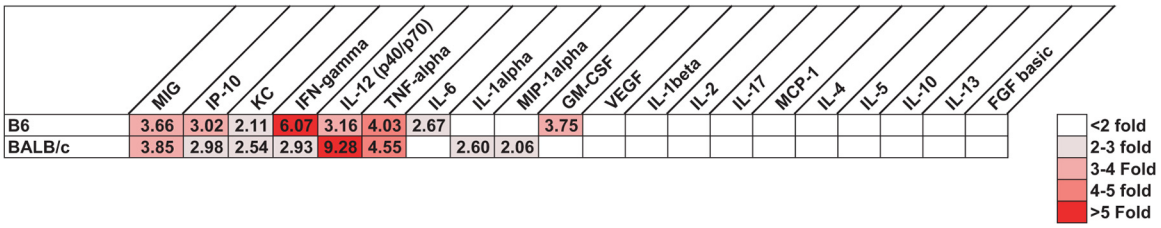

FIG 4 LVS *clpB* induces a proinflammatory response in the lung early after infection. B6 or BALB/c mice were intranasally inoculated with LVS (5×10^2 CFU) or LVS *clpB* (5×10^4 CFU) or left uninfected. At 3 days postinoculation, BALF was collected, and cytokine and chemokine concentrations were determined by using a Luminex-based assay. Cytokine and chemokines levels were first normalized to the levels in uninfected mice, and the fold increase in cytokine or chemokine concentrations from LVS *clpB*-infected mice over LVS-infected mice was then determined for each infected group; values are indicated in boldface type if they exceeded 2-fold ($n = 4$ to 7 mice/group). Data are combined from at least 2 independent experiments per mouse strain. ANOVA with Tukey's posttest was used to determine significant changes in cytokine and chemokine concentrations within each mouse strain. LVS *clpB* levels were significantly higher ($P \leq 0.05$) than LVS levels in both mouse strains for IP-10, KC, IL-12, and TNF-α. LVS *clpB* levels were significantly higher ($P \leq 0.05$) than LVS levels in B6 mice for IFN-γ, IL-6, and GM-CSF. LVS *clpB* levels were significantly higher ($P \leq 0.05$) than LVS levels in BALB/c mice for MIG.

matory cytokines and chemokines in the lungs of BALB/c mice on day 3 postinoculation, whereas LVS did not (Fig. 4). BALB/c mice also had significantly higher day 3 postinoculation lung LVS burdens than LVS *clpB* (see Fig. S6 in the supplemental material). Clearly, LVS *clpB* failed to suppress early proinflammatory cytokine production in the lung, which is in stark contrast to LVS infection, which does not induce proinflammatory cytokine production in the lung (Fig. 4) (11). Additionally, the failure of LVS *clpB* to suppress proinflammatory cytokine production is not specific to a particular mouse strain, as the same effect was seen in B6 and BALB/c mice. Despite the high-inoculum dose of LVS *dotU*, this strain did not elicit any detectable proinflammatory cytokine production in the lungs of infected B6 or BALB/c mice (data not shown).

Depletion of IFN-γ early after LVS *clpB* inoculation increases bacterial burdens. To confirm that proinflammatory cytokine production early after inoculation was important for innate immunity-mediated bacterial clearance, we treated B6 mice with 500 μg of XMG1.2 (anti-IFN-γ) or rat IgG1 isotype antibody on day 0 and day 2 postinoculation. On day 3 postinoculation, mice were sacrificed, and bacterial burdens in the spleen, liver, and lung were determined. Mice receiving IFN-γ-depleting antibody had significantly higher bacterial burdens in all organs than mice receiving isotype control antibody (see Fig. S7A to S7C in the supplemental material). We confirmed IFN-γ depletion by subjecting clarified tissue homogenates to Luminex analysis. All mice receiving anti-IFN-γ depleting antibody had IFN-γ levels below the detection limit, whereas isotype control animals had high levels of lung IFN-γ (see Fig. S7D in the supplemental material). These data indicate that proinflammatory cytokine production, such as IFN-γ, early after LVS *clpB* inoculation helps control bacterial replication.

Adaptive immunity is required for LVS *clpB* clearance. LVS clearance requires adaptive immunity (15). Because LVS *clpB* induced a robust innate immune response and was nearly cleared from the host prior to the peak of the adaptive immune response (day 10 postinoculation [19]), this raised the possibility that the innate immune system was capable of controlling the infection and mediating bacterial clearance without the requirement of adaptive immunity, even though the adaptive response was vigorous (see below). To test this possibility, we infected B6 and Rag$^{-/-}$ mice with 5×10^4 CFU LVS *clpB*. On days 3 and 7 postinfection, B6 and Rag$^{-/-}$ mice had equivalent bacterial burdens in the lung, indicating that innate immunity was capable of controlling the infection initially (Fig. 5A). We next infected Rag$^{-/-}$ and B6 mice with 5×10^4 CFU LVS *clpB* and harvested organs at 28 days postinoculation. No bacteria were recovered from the B6 mice, but LVS *clpB* persisted in the lungs of Rag$^{-/-}$ mice (Fig. 5A). The same trend was seen for the spleen and liver (data not shown). Despite persistent bacteremia with LVS *clpB* in Rag$^{-/-}$ mice, weight loss profiles were identical for Rag$^{-/-}$ and B6 mice (Fig. 5B). Since LVS *clpB* persisted in Rag$^{-/-}$ mice, this result indicates that adaptive immunity is required for LVS *clpB* clearance, similar to LVS (15); the robust innate response is not sufficient to clear LVS *clpB*. This further suggests that the innate immune response is responsible for the weight loss profile observed for LVS *clpB*-inoculated mice.

LVS *clpB* infection induces altered immune expansion. After determining that adaptive immunity is required for LVS *clpB* clearance, we characterized the adaptive immune response to this

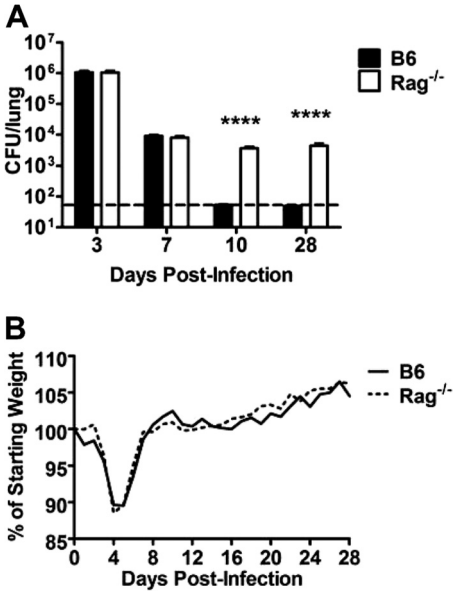

FIG 5 Adaptive immunity is required for LVS *clpB* clearance. B6 or Rag$^{-/-}$ mice were intranasally inoculated with 5×10^4 CFU LVS *clpB*. (A) Bacterial burdens were determined in the lung on days 3, 7, 10, and 28 postinoculation by plating serial dilutions of organ homogenate onto chocolate agar ($n = 6$ to 8 mice/group). Data are combined from 2 independent experiments. The dashed line indicates the limit of detection of 50 CFU. Statistical significance was determined on log-transformed data by using Student's *t* test. (B) Mouse weight was determined daily and is reported as a percentage of the starting weight ($n = 6$ to 8 mice/group). Data are combined from 2 independent experiments.

strain. First, we determined the total number of cells recovered from the spleen and lung on days 7 and 10 postinoculation (Fig. 6). LVS- and LVS *clpB*-infected mice had similar increases in spleen cellularity, with an approximately 2- to 3-fold increase in the total number of cells compared to uninfected mice on days 7 and 10 postinoculation (Fig. 6A and B). LVS- and LVS *clpB*-infected mice also had increased lung cellularity of 2- to 5-fold over that of uninfected mice on days 7 and 10 postinoculation (Fig. 6C and D). When spleen cellularity of LVS- and LVS *clpB*-infected mice was compared, there was no significant difference on day 7 or 10 postinoculation (Fig. 6A and B). However, lung cellularity was decreased significantly in LVS *clpB*-infected mice compared to LVS-infected mice on days 7 and 10 postinoculation (Fig. 6C and D). The difference in lung cellularity is likely due to the contraction of the immune response following LVS *clpB* clearance. While the LVS *clpB* infection was nearly cleared on day 10 postinoculation, LVS-infected mice still had high bacterial burdens, and an ongoing infection likely drives sustained lung cellularity. Because LVS *dotU* failed to grow *in vivo*, it was not surprising that LVS *dotU*-infected mice did not have any increase in spleen or lung cellularity compared to uninfected mice and exhibited no immune expansion from days 7 to 10 (Fig. 6A to D).

LVS *clpB* infection induced a robust IFN-γ-mediated immune response similar in magnitude to that induced by LVS infection. Given the strong innate response, we suspected that in spite of the earlier clearance of LVS *clpB*, we would still observe a robust adaptive response. We therefore examined whether IFN-γ production by CD4$^+$ T cells was altered after LVS *clpB* infection (Fig. 7A to D). We identified IFN-γ-producing T cells using intra-

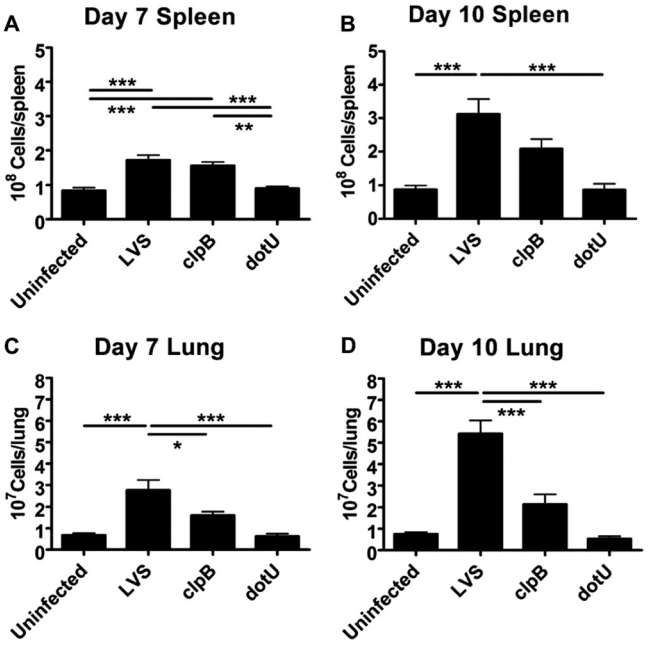

FIG 6 LVS and LVS *clpB* infection leads to increased spleen and lung cellularity. B6 mice were intranasally inoculated with LVS (5×10^2 CFU), LVS *clpB* (5×10^4 CFU), or LVS *dotU* (5×10^5 CFU) or left uninfected. The total number of cells in the spleen or lung was determined on days 7 and 10 postinoculation by trypan blue exclusion ($n = 4$ to 9 mice/group). Data are combined from at least 4 independent experiments. Statistical significance was determined by using an ANOVA with Tukey's posttest. (A) Total number of cells in the spleen on day 7 postinoculation. (B) Total number of cells in the spleen on day 10 postinoculation. (C) Total number of cells in the lung on day 7 postinoculation. (D) Total number of cells in the lung on day 10 postinoculation.

cellular cytokine staining following coculture with LVS-infected congenic B6-CD45.1 splenocytes as antigen-presenting cells. The gating scheme used for all flow cytometry analyses is shown in Fig. S1 in the supplemental material. We found no statistically significant difference in the number of $CD4^+$ T cells producing IFN-γ in the spleen and lung in LVS- and LVS *clpB*-infected mice on day 7 (Fig. 7A and B). On day 10 postinoculation, the number of splenic $CD4^+$ IFN-γ^+ T cells was not significantly different between LVS- and LVS *clpB*-infected mice in spite of lower bacterial burdens in LVS *clpB*-infected mice (Fig. 7C). In the lung, however, there was a significant decrease in the number of $CD4^+$ IFN-γ^+ T cells in LVS *clpB*-infected mice compared to LVS-infected mice (Fig. 7D). While the frequency of IFN-γ^+ cells in the $CD4^+$ T cell pool in LVS *clpB*-infected mice was higher than that in LVS-infected mice (41.6% versus 35.8%), the difference did not reach statistical significance. Because the frequency of IFN-γ^+ cells of $CD4^+$ T cells was similar in the lungs of LVS- and LVS *clpB*-infected mice, the difference in the absolute number was due to fewer total cells in the lungs of LVS *clpB*-infected mice on day 10 postinoculation (Fig. 6D). We did not detect an increase in the number of splenic or lung $CD4^+$ IFN-γ^+ cells in LVS *dotU*-infected mice compared to uninfected mice (Fig. 7A to D).

$CD8^+$ T cells showed a pattern of IFN-γ production similar to that of $CD4^+$ T cells (Fig. 7E to H). There was no statistical difference in the number of $CD8^+$ IFN-γ^+ T cells in the spleen or lungs of LVS- and LVS *clpB*-infected mice on day 7 postinoculation (Fig. 7E and F). On day 10 postinoculation, there were equivalent numbers of $CD8^+$ T cells producing IFN-γ in the spleens of LVS *clpB*- and LVS-infected mice (Fig. 7G). There was, however, a significant decrease in the number of IFN-γ^+ $CD8^+$ T cells in the lungs of LVS *clpB*-infected mice on day 10 postinoculation compared to LVS-infected mice (Fig. 7H). Again, the percentages of IFN-γ^+

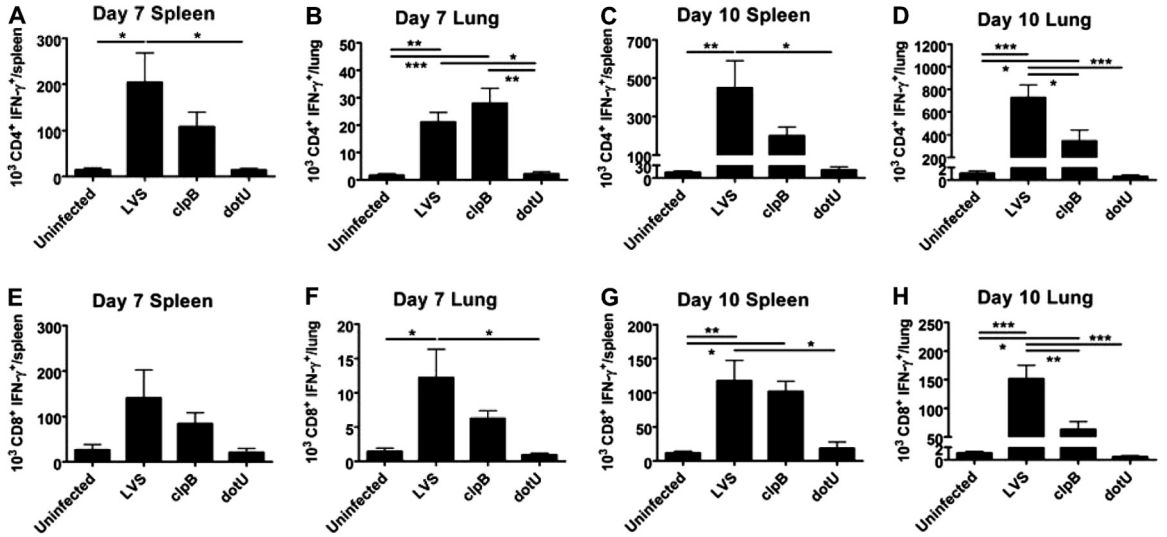

FIG 7 LVS and LVS *clpB* infection leads to increased IFN-γ^+ $CD4^+$ and $CD8^+$ T cells. B6 mice were intranasally inoculated with LVS (5×10^2 CFU), LVS *clpB* (5×10^4 CFU), or LVS *dotU* (5×10^5 CFU) or left uninfected. On days 7 and 10 postinoculation, splenocytes or isolated lung cells were restimulated with LVS-infected B6-CD45.1 antigen-presenting cells for 24 h. Brefeldin A was added during the last 4 h of coculture ($n = 4$ to 9 mice/group). Data are combined from at least 4 independent experiments. Statistical significance was determined by using an ANOVA with Tukey's posttest. (A) Number of IFN-γ-producing $CD4^+$ cells in the spleen at 7 days postinoculation. (B) Number of IFN-γ-producing $CD4^+$ cells in the lung at 7 days postinoculation. (C) Number of IFN-γ-producing $CD4^+$ cells in the spleen on day 10 postinoculation. (D) Number of IFN-γ-producing $CD4^+$ cells in the lung on day 10 postinoculation. (E) Number of IFN-γ-producing $CD8^+$ cells in the spleen at 7 days postinoculation. (F) Number of IFN-γ-producing $CD8^+$ cells in the lung at 7 days postinoculation. (G) Number of IFN-γ-producing $CD8^+$ cells in the spleen on day 10 postinoculation. (H) Number of IFN-γ-producing $CD8^+$ cells in the lung on day 10 postinoculation.

cells in the $CD8^+$ T cell pool remained the same; therefore, any decrease in absolute number on day 10 is due to decreased lung cellularity in LVS *clpB*-infected mice. Uninfected and LVS *dotU*-infected mice were similar to each other in terms of the absolute number of $CD8^+$ IFN-γ^+ cells in the spleen and lungs on days 7 and 10 postinoculation (Fig. 7E to H).

We found an approximately 2-fold increase in the number of IFN-γ^+ $CD4^+$ T cells in the spleens of LVS- and LVS *clpB*-infected mice between days 7 and 10 postinoculation (Fig. 7A and C). There was at least a 10-fold expansion of IFN-γ^+ $CD4^+$ T cells in the lungs of LVS- and LVS *clpB*-infected mice between days 7 and 10 postinoculation (Fig. 7B and D). LVS *clpB*-infected mice, however, did not show the degree of expansion seen in LVS-infected mice (10-fold versus 35-fold). There was no change in the number of IFN-γ^+ $CD8^+$ T cells in the spleens of LVS- or LVS *clpB*-infected mice between days 7 and 10 postinoculation (Fig. 7E and G). There was, however, an approximately 10-fold increase in the number of responding IFN-γ^+ $CD8^+$ T cells in the lungs of both LVS- and LVS *clpB*-infected mice between days 7 and 10 (Fig. 7F and H). Together, these results indicate that LVS *clpB* infection induced a frequency of IFN-γ^+ $CD4^+$ and $CD8^+$ T cells similar to that induced by LVS infection.

LVS *clpB* infection led to increased IFN-γ expression by responding T cells compared to LVS infection. We next measured the mean fluorescence intensity (MFI) of $CD4^+$ IFN-γ^+ cells because MFI is an indication of how much IFN-γ is expressed on a per-cell basis. We normalized the data by subtracting the MFI of the IFN-γ-negative population from the MFI of the IFN-γ-positive population to give a change in MFI (ΔMFI). Figure 8A to D shows data for $CD4^+$ IFN-γ^+ ΔMFI combined from 4 independent experiments. The differences in ΔMFI for $CD4^+$ IFN-γ^+ T cells on day 10 were consistent from experiment to experiment, and representative histograms derived from the same experiment are shown (Fig. 8E to H). There was a significant increase in the ΔMFI of $CD4^+$ cells producing IFN-γ in the spleens and lungs from LVS- and LVS *clpB*-infected mice compared to uninfected mice on day 7 and 10 postinoculation (Fig. 8A to D). On day 7 postinoculation, there was no significant difference in $CD4^+$ IFN-γ ΔMFI from LVS-infected mice compared to LVS *clpB*-infected mice in both the spleen and lung (Fig. 8A and B). However, on day 10, there was a significant increase in IFN-γ ΔMFI from LVS *clpB*-infected mice compared to LVS-infected mice in both the spleen and lung (Fig. 8C and D). To further investigate IFN-γ production by $CD4^+$ T cells, we enriched $CD4^+$ T cells from the spleen and lung on day 10 postinoculation. We chose day 10 because this time point had more responding $CD4^+$ T cells than at day 7 and also exhibited differences in IFN-γ expression, as measured by ΔMFI. Enriched lung and spleen $CD4^+$ T cells were restimulated by using LVS-infected T cell-depleted splenocytes. The concentration of IFN-γ in the culture supernatant was determined by ELISA 24 h after the start of the coculture and was normalized to the number of $CD4^+$ T cells in each sample (see Fig. S8 in the supplemental material). There was no difference in the IFN-γ concentration following restimulation of enriched lung or spleen $CD4^+$ T cells from LVS- or LVS *clpB*-infected mice. It is possible that we did not see the difference in IFN-γ production by $CD4^+$ T cells because of IFN-γ turnover during the culture. Additionally, intracellular cytokine staining is a much more sensitive technique than ELISA of culture supernatants.

The IFN-γ ΔMFI trend for $CD8^+$ T cells is similar to that for the $CD4^+$ T cell subset. Representative histograms derived from the same experiment for IFN-γ^+ $CD8^+$ T cells from LVS- and LVS *clpB*-infected mice are shown (Fig. 8M to P). Measurement of IFN-γ ΔMFI in the spleen and lung showed similar expression levels of IFN-γ at 7 days postinoculation in LVS- and LVS *clpB*-infected mice (Fig. 8I and J). There was a significant increase in the ΔMFI of IFN-γ^+ cells in the $CD8^+$ T cell pool in the spleen and lung in LVS *clpB*-infected mice compared to LVS-infected mice on day 10 postinoculation (Fig. 8K and L). The IFN-γ ΔMFI in $CD8^+$ T cells indicates that like $CD4^+$ T cells, the cells from LVS *clpB*-infected mice express more IFN-γ than do cells isolated from LVS-infected mice, even though fewer cells are present.

LVS *clpB* infection increases IL-17 expression levels compared to LVS infection. Th17 cells are also involved in the immune response during pneumonic tularemia (19, 20). Although there was no significant change at day 7 postinoculation, by day 10 postinoculation, there was a significant increase in the absolute number of $CD4^+$ IL-$17A^+$ T cells in the lungs of LVS-infected mice compared to uninfected mice (Fig. 9C and D). LVS *clpB*-infected mice trended toward more $CD4^+$ IL-$17A^+$ T cells in the lungs on day 10 postinoculation than in uninfected mice, but the difference did not reach statistical significance (Fig. 9D). There was no significant difference in the absolute number of Th17 cells in the lungs of LVS- and LVS *clpB*-infected mice on day 10 postinoculation (Fig. 9D). There was also an expansion of Th17 cells in the lung between days 7 and 10 postinoculation for LVS- and LVS *clpB*-infected mice, with nearly a 10-fold increase in cell number (Fig. 9C and D). Interestingly, there was a significant increase of IL-17A ΔMFI in the lung of LVS *clpB*-infected mice on day 10 postinoculation compared to LVS-infected mice (Fig. 9H). The absolute number of splenic $CD4^+$ T cells producing IL-17A was similar on days 7 and 10 postinoculation among uninfected and LVS-, LVS *clpB*-, and LVS *dotU*-infected mice, indicating that Th17 cells are not responding to infection in the spleen (Fig. 9A and B). There was also no significant difference in the splenic IL-17A ΔMFI when all groups of mice were compared (Fig. 9E and F). We also determined IL-17 secretion by enriched $CD4^+$ T cells from the lung and spleen on day 10. These cells were restimulated with LVS-infected, T cell-depleted splenocytes, and the concentration of IL-17 was determined by ELISA (see Fig. S9 in the supplemental material). Enriched $CD4^+$ T cells from the lungs of LVS- and LVS *clpB*-infected mice secreted similar amounts of IL-17. Overall, our results suggest that Th17 expansion occurs largely at the site of primary infection.

Altogether, our results demonstrate that LVS *clpB* infection induces altered host immunity compared to wild-type LVS infection. First, we saw early proinflammatory cytokine production in the lungs of LVS *clpB*-infected mice, a process that was inhibited during LVS infection. Additionally, LVS *clpB*-infected mice produced an expansion of Th1, Th17, and $CD8^+$ T cell responses at least equivalent to that of LVS-infected mice, with lower bacterial burdens and a shorter duration of infection.

DISCUSSION

Bacterial attenuation can be the consequence of a strain's failure to grow, as in the case of auxotrophs, or a strain's failure to inhibit components of host immunity. Both *in vitro* and *in vivo* screens have identified *Francisella* virulence determinants, and several of those screens identified *clpB* as a gene required for virulence (5–7, 36). While several groups described a slight intracellular growth

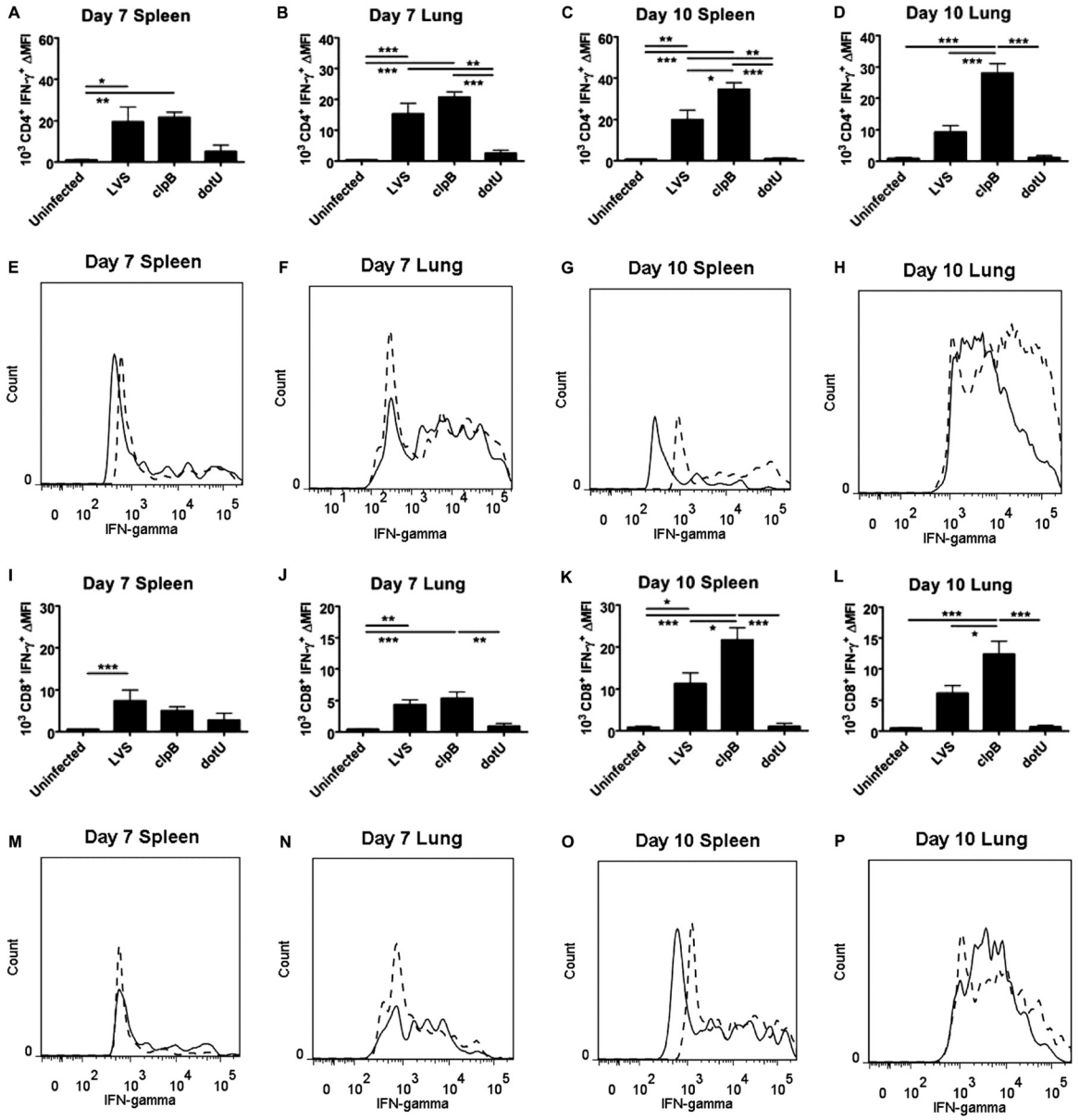

FIG 8 $CD4^+$ and $CD8^+$ T cells from LVS *clpB*-infected mice express more IFN-γ per cell than do those from LVS-infected mice. B6 mice were intranasally inoculated with LVS (5×10^2 CFU), LVS *clpB* (5×10^4 CFU), or LVS *dotU* (5×10^5 CFU) or left uninfected. On days 7 and 10 postinfection, splenocytes or isolated lung cells were restimulated with LVS-infected B6-CD45.1 antigen-presenting cells for 24 h. Brefeldin A was added during the last 4 h of coculture. To determine the relative mean fluorescent intensity (ΔMFI) for each sample, the MFI of the IFN-γ-negative population was subtracted from the MFI of the IFN-γ-positive population ($n = 4$ to 9 mice/group). Data are combined from at least 4 independent experiments. Statistical significance was determined by using an ANOVA with Tukey's posttest. (A) IFN-γ ΔMFI for $CD4^+$ T cells in the spleen at 7 days postinoculation. (B) IFN-γ ΔMFI for $CD4^+$ T cells in the lung at 7 days postinoculation. (C) IFN-γ ΔMFI for $CD4^+$ T cells in the spleen at 10 days postinoculation. (D) IFN-γ ΔMFI for $CD4^+$ T cells in the lung at 10 days postinoculation. (E) Representative histograms of the IFN-γ^+ $CD4^+$ T cells from LVS (solid line)- and LVS *clpB* (dotted line)-infected mice in the spleen on day 7 postinoculation. (F) Representative histograms of the IFN-γ^+ $CD4^+$ T cells from LVS (solid line)- and LVS *clpB* (dotted line)-infected mice in the lung on day 7 postinoculation. (G) Representative histograms of the IFN-γ^+ $CD4^+$ T cells from LVS (solid line)- and LVS *clpB* (dotted line)-infected mice in the spleen on day 10 postinoculation. (H) Representative histograms of the IFN-γ^+ $CD4^+$ T cells from LVS (solid line)- and LVS *clpB* (dotted line)-infected mice in the lung on day 10 postinoculation. (I) IFN-γ ΔMFI for $CD8^+$ T cells in the spleen at 7 days postinoculation. (J) IFN-γ ΔMFI for $CD4^+$ T cells in the lung at 7 days postinoculation. (K) IFN-γ ΔMFI for $CD8^+$ T cells in the spleen at 10 days postinoculation. (L) IFN-γ ΔMFI for $CD8^+$ T cells in the lung at 10 days postinoculation. (M) Representative histograms of the IFN-γ^+ $CD8^+$ T cells from LVS (solid line)- and LVS *clpB* (dotted line)-infected mice in the spleen on day 7 postinoculation. (N) Representative histograms of the IFN-γ^+ $CD8^+$ T cells from LVS (solid line)- and LVS *clpB* (dotted line)-infected mice in the lung on day 7 postinoculation. (O) Representative histograms of the IFN-γ^+ $CD8^+$ T cells from LVS (solid line)- and LVS *clpB* (dotted line)-infected mice in the spleen on day 10 postinoculation. (P) Representative histograms of the IFN-γ^+ $CD8^+$ T cells from LVS (solid line)- and LVS *clpB* (dotted line)-infected mice in the lung on day 10 postinoculation.

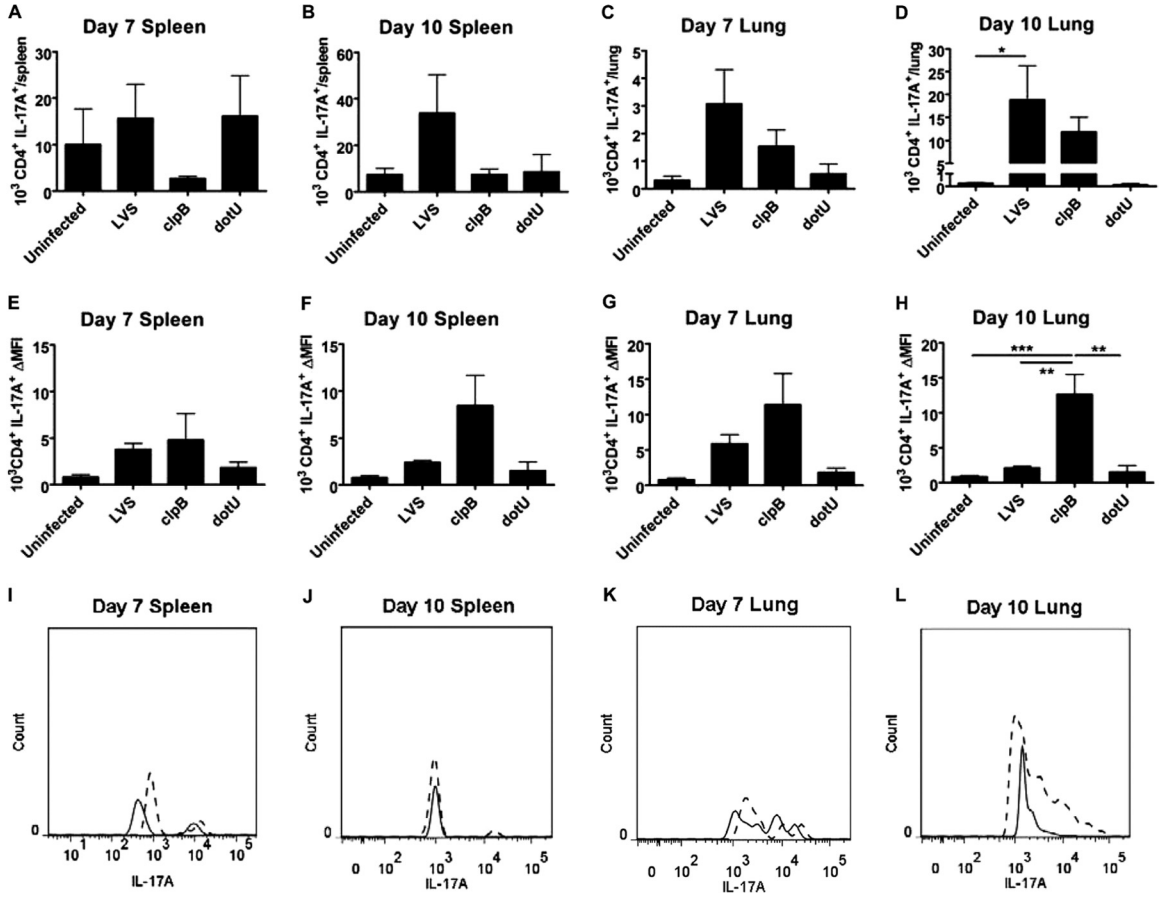

FIG 9 Th17 cells from LVS *clpB*-infected mice express more IL-17 than do cells from LVS-infected mice. B6 mice were intranasally inoculated with LVS (5×10^2 CFU), LVS *clpB* (5×10^4 CFU), or LVS *dotU* (5×10^5 CFU) or left uninfected. On days 7 and 10 postinoculation, splenocytes or isolated lung cells were restimulated with LVS-infected B6-CD45.1 antigen-presenting cells for 24 h. Brefeldin A was added during the last 4 h of coculture. To determine relative mean fluorescence intensity (ΔMFI), the MFI of the IL-17A-negative population was subtracted from the MFI of the IL-17A-positive population ($n = 4$ to 9 mice/group). Data are combined from at least 4 independent experiments. Statistical significance was determined by using an ANOVA with Tukey's posttest. (A) Number of IL-17A-producing $CD4^+$ cells in the spleen on day 7 postinoculation. (B) Number of IL-17A-producing $CD4^+$ cells in the spleen on day 10 postinoculation. (C) Number of IL-17A-producing $CD4^+$ cells in the lung on day 7 postinoculation. (D) Number of IL-17A-producing $CD4^+$ cells in the lung on day 10 postinoculation. (E) IL-17A ΔMFI for $CD4^+$ T cells in the spleen at 7 days postinoculation. (F) IL-17A ΔMFI for $CD4^+$ T cells in the spleen at 10 days postinoculation. (G) IL-17A ΔMFI for $CD4^+$ T cells in the lung at 7 days postinoculation. (H) IL-17A ΔMFI for $CD4^+$ T cells in the lung at 10 days postinoculation. (I) Representative histograms of the IL-17A$^+$ $CD4^+$ T cells from LVS (solid line)- and LVS *clpB* (dotted line)-infected mice in the spleen on day 7 postinoculation. (J) Representative histograms of the IL-17A$^+$ $CD4^+$ T cells from LVS (solid line)- and LVS *clpB* (dotted line)-infected mice in the spleen on day 10 postinoculation. (K) Representative histograms of the IL-17A$^+$ $CD4^+$ T cells from LVS (solid line)- and LVS *clpB* (dotted line)-infected mice in the lung on day 7 postinoculation. (L) Representative histograms of the IL-17A$^+$ $CD4^+$ T cells from LVS (solid line)- and LVS *clpB* (dotted line)-infected mice in the lung on day 10 postinoculation.

defect for *clpB* strains (23, 37, 38), we did not see an intracellular growth defect for our LVS *clpB* strains in the cell types that we tested. This result suggested that something else was responsible for the attenuation of *clpB* in animal models of infection (23–25). We therefore hypothesized that LVS *clpB* induces an altered immune response that mediates faster bacterial clearance.

To test our hypothesis, we first confirmed that our LVS *clpB* strain was attenuated in a pneumonic model of tularemia. In order to achieve similar bacterial burdens early after infection, we inoculated mice with a 100-fold-higher dose of LVS *clpB* than of LVS. Ideally, we would have used the same inoculation dose for both bacterial strains. However, not only did LVS *clpB* fail to disseminate to the spleen and liver in all mice, the bacterial burdens were also significantly lower in all organs tested on day 3 postinoculation at an inoculation dose of 5×10^2 CFU. An inoculation dose of 5×10^4 CFU of LVS *clpB* led to bacterial burdens similar to those of LVS at 3 days postinoculation and allowed us to examine differences in the adaptive immune response in the absence of large differences in the overall antigen load. Despite similar bacterial burdens early after inoculation, we observed rapid clearance of LVS *clpB*. Even though LVS *clpB* was cleared rapidly from the host, this strain did elicit an adaptive immune response that developed into protective memory. Importantly, previous infection with LVS *clpB* provided protection equivalent to that provided by LVS against subsequent lethal LVS intranasal inoculation. The bacterial burdens in LVS- and LVS *clpB*-vaccinated mice infected 120 days after vaccination were higher than those in the same groups challenged 28 days after vaccination. The increase in bacterial burden was consistent with the increased weight loss seen when mice were challenged 120 days after vaccination. Because the number of

antigen-specific T cells decreases over time, we hypothesize that the increased bacterial burdens seen upon challenge 120 days after vaccination were due to fewer responding T cells than those at day 28. However, we cannot directly address this hypothesis by quantifying the number of *Francisella*-specific T cells because major histocompatibility complex class I (MHCI) or MHCII tetramer is not yet available. Previous LVS *clpB* infection did not provide complete protection against aerosolized SchuS4 administered 28 days after LVS *clpB* infection. LVS *clpB* infection did, however, increase the median survival time. One mouse previously inoculated with LVS *dotU* survived lethal LVS challenge; however, we do not know if this was the result of a secondary immune response. This result was surprising given that our intracellular cytokine staining showed that LVS *dotU*-infected mice behaved much like naïve mice, with similar low numbers of IFN-γ-producing T cells. However, LVS *dotU* persisted intracellularly in some mice until at least day 7 postinoculation, allowing time for a *F. tularensis*-specific T cell response to be primed. The protection was incomplete and indicates that a LVS *dotU* mutant would not be an effective vaccine. Overall, our LVS *clpB* strain was attenuated in pneumonic tularemia while providing 100% protection against subsequent lethal infection, just as other groups have shown by using other models of tularemia (23–25).

After confirming the attenuation of LVS *clpB* in pneumonic tularemia, we examined the innate immune response in the lung. LVS infection does not elicit a proinflammatory cytokine response in the lung despite promoting phenotypic maturation of dendritic cells (11). We also found that LVS infection did not elicit a proinflammatory cytokine response in the lung despite very high bacterial burdens on day 3 postinoculation. LVS *clpB*, in contrast, did elicit a robust proinflammatory cytokine response in the lungs of both B6 and BALB/c mice. The failure of LVS *clpB* to inhibit early cytokine production could explain why lower inoculation doses resulted in poor dissemination to the spleen and liver. Because antibody depletion of IFN-γ increased lung LVS *clpB* burdens, these data suggest that the high concentrations of proinflammatory cytokines and chemokines in the lung are responsible for the decrease in bacterial burdens compared to LVS burdens that we observed on day 3 postinoculation.

Despite a robust proinflammatory innate immune response to LVS *clpB*, the innate response was not sufficient to mediate bacterial clearance alone. Additionally, we knew from our protection studies that there was priming of the adaptive immune response because mice previously infected with LVS *clpB* were protected from lethal LVS challenge. We then began to characterize the adaptive immune response to LVS *clpB*. When overall immune expansion was compared, LVS and LVS *clpB* infection led to a similar increase in the number of cells found in the spleen on days 7 and 10. We found a significant decrease in the number of cells isolated from the lungs of LVS *clpB*-infected mice on days 7 and 10 postinoculation compared to LVS-infected mice. This decrease was likely due to contraction of the immune response, as LVS *clpB* was rapidly cleared from the host, while LVS-infected mice maintained high bacterial burdens. To further support this, the percentages of $CD4^+$ and $CD8^+$ T cells in the lungs were the same in LVS- and LVS *clpB*-infected mice, indicating that while the magnitude of the response was changing, the composition of the response remained unchanged. When we examined the effector function of cells in the spleen, we found equivalent numbers of $CD4^+$ and $CD8^+$ T cells producing IFN-γ in LVS- and LVS *clpB*-infected mice. The absolute number of $CD4^+$ and $CD8^+$ T cells in the lung of LVS *clpB*-infected mice was decreased compared to that in lungs of LVS-infected mice, but the percentage of cells producing IFN-γ remained the same.

Although we found similar frequencies of IFN-γ-producing $CD4^+$ and $CD8^+$ T cells after LVS or LVS *clpB* infection, we did find altered expression levels of IFN-γ, as measured by ΔMFI. There was a significant increase in the amount of IFN-γ expressed by T cells from LVS *clpB*-infected mice compared to LVS-infected mice in both the spleen and lung, as measured by ΔMFI. Since IFN-γ is critical for LVS clearance, and administration of recombinant IFN-γ decreased bacterial burdens, the increased production of IFN-γ by T cells in LVS *clpB*-infected mice is consistent with faster clearance of LVS *clpB* (18).

The IL-17 response is also important during pneumonic tularemia. We have previously shown that LVS intranasal, but not intradermal, inoculation induces Th17 cells in the lung (19). IL-17 production following *F. tularensis* infection has been shown to promote IL-12 production by dendritic cells and to indirectly promote a Th1 immune response (20). Although infection with LVS or LVS *clpB* led to similar numbers of Th17 cells in the lungs of infected mice, Th17 cells from LVS *clpB*-infected mice expressed significantly more IL-17A, as measured by ΔMFI. The increase in IL-17 expression by LVS *clpB*-infected mice is consistent with findings reported previously by Lin et al., where the Th1 response was promoted by IL-17 (20).

We also measured IFN-γ and IL-17 concentrations in the BALF at 7 and 10 days postinoculation. We did not detect increased concentrations of either cytokine in BALF from LVS *clpB*-infected mice compared to LVS-infected mice. Although these data are not in agreement with the flow ΔMFI data, we attribute the difference to differential distribution of immune cells between the airspace and lung parenchyma. Cytokines in the BALF are secreted predominantly by cells within the airspace and represent production by a variety of immune cells. In contrast, our intracellular cytokine staining experiments measured IFN-γ and IL-17 in the entire lung, but this analysis was limited to T cells only. When we enriched $CD4^+$ T cells from the lung and spleen on day 10 postinoculation and restimulated them *ex vivo* with LVS-infected T cell-depleted splenocytes, we did not detect differences in IFN-γ or IL-17A secretion into the culture supernatant. Differences between the readout of the flow cytometry analysis and ELISAs could also account for disparate results. At a minimum, however, $CD4^+$ T cells isolated from LVS *clpB*-infected mice are able to produce equivalent amounts of cytokine compared to T cells from LVS-infected mice.

The increase in IFN-γ production by T cells in LVS *clpB*-infected mice could be caused by differences in lung prostaglandin E_2 (PGE_2) concentrations. PGE_2 suppresses IFN-γ production by T cells in LVS-infected mice (19). U112 *clpB* fails to induce PGE_2 in BMDMs (35), and LVS *clpB* induced significantly less PGE_2 than did wild-type LVS in BMDMs (data not shown). LVS *clpB*-infected mice had significantly lower PGE_2 concentrations in the lavage fluid on days 7 and 10 postinoculation than did LVS-infected mice (data not shown). The high concentration of PGE_2 in LVS-infected mice decreased IFN-γ production by responding T cells, an inhibitory process not present in LVS *clpB*-infected mice. The increased IFN-γ production in LVS *clpB*-infected mice is also consistent with increased IL-17 expression by T cells in LVS *clpB*-infected mice based on the finding by Lin et al. that the Th1 re-

sponse was promoted by IL-17 (20). However, PGE_2 has been shown to promote IL-23 production, which drives the development of Th17 cells (39–42). In LVS *clpB*-infected mice, there was little PGE_2 present in the BALF, suggesting that there is another mechanism driving Th17 accumulation, since this cell subset was present in equivalent numbers in LVS- and LVS *clpB*-infected mice despite dramatic differences in PGE_2 levels.

Although we are still in the process of identifying the *F. tularensis* effector molecule responsible for inducing PGE_2, it seems unlikely that ClpB directly induces PGE_2. ClpB is an intracellular chaperone protein that is unlikely to be sensed by the host. A previous proteomic analysis by Meibom et al. of a membrane-enriched protein fraction from a LVS *clpB* mutant identified 5 proteins with decreased expression levels compared to LVS under conditions of elevated temperature (23). None of the identified targets of ClpB are required for PGE_2 induction (35); therefore, ClpB must have another target that is involved in PGE_2 induction. We speculate that *clpB* was identified as a gene necessary for PGE_2 induction because ClpB plays a role in assembly of the type VI secretion system that is responsible for secreting the unknown PGE_2 inducer. Studies to identify the mechanism(s) utilized by *F. tularensis* to induce PGE_2 synthesis are ongoing.

ClpB is a highly conserved chaperone protein present not only in prokaryotes but also in eukaryotes and plants (43). Due to ClpB's conserved nature and the finding that disruption of *clpB* attenuates *F. tularensis* as well as other bacteria (44–48), this gene is an excellent candidate target for attenuation of pathogenic bacteria for vaccine development. In the case of *F. tularensis*, LVS *clpB* infection was cleared faster than LVS yet induced a robust IFN-γ-mediated immune response that was protective in both short- and long-term secondary infections. Therefore, *clpB* serves as an advantageous target for *F. tularensis* attenuation for future vaccine development. This work also highlights the importance of examining the immune response to attenuated mutants, particularly in the course of vaccine development.

ACKNOWLEDGMENTS

We thank H.-J. Wu, Kurt Griffin, and Michael Kuhns for helpful conversations and review of the manuscript. We also thank Paula Campbell and the University of Arizona Flow Cytometry Core Facility. Biomarker profiling was performed in the Duke Human Vaccine Institute/Regional Biocontainment Laboratory Biomarker Analysis Shared Resource Facility (Durham, NC) by Kristina Riebe.

Select studies were performed in the Regional Biocontainment Laboratory at Duke, which received partial support for construction from the National Institute of Allergy and Infectious Diseases, National Institutes of Health (grant UC6-AI058607). This work was supported by National Institutes of Health grant R01 AI078345 and National Institute of Allergy and Infectious Diseases Southeast Regional Center of Excellence for Emerging Infections and Biodefense grant U54 AI057157.

The contents of this work are solely the responsibility of the authors and do not necessarily represent the official views of the NIH.

REFERENCES

1. **Pechous RD, McCarthy TR, Zahrt TC.** 2009. Working toward the future: insights into Francisella tularensis pathogenesis and vaccine development. Microbiol. Mol. Biol. Rev. **73**:684–711.
2. **Dennis DT, Inglesby TV, Henderson DA, Bartlett JG, Ascher MS, Eitzen E, Fine AD, Friedlander AM, Hauer J, Layton M, Lillibridge SR, McDade JE, Osterholm MT, O'Toole T, Parker G, Perl TM, Russell PK, Tonat K.** 2001. Tularemia as a biological weapon: medical and public health management. JAMA **285**:2763–2773.
3. **Christopher GW, Cieslak TJ, Pavlin JA, Eitzen EM, Jr.** 1997. Biological warfare. A historical perspective. JAMA **278**:412–417.
4. **Alibek K, Handelman S.** 1999. Biohazard: the chilling true story of the largest covert biological weapons program in the world, told from the inside by the man who ran it, 1st ed. Random House, New York, NY.
5. **Kadzhaev K, Zingmark C, Golovliov I, Bolanowski M, Shen H, Conlan W, Sjostedt A.** 2009. Identification of genes contributing to the virulence of Francisella tularensis SCHU S4 in a mouse intradermal infection model. PLoS One **4**:e5463. doi:10.1371/journal.pone.0005463.
6. **Su J, Yang J, Zhao D, Kawula TH, Banas JA, Zhang JR.** 2007. Genome-wide identification of Francisella tularensis virulence determinants. Infect. Immun. **75**:3089–3101.
7. **Weiss DS, Brotcke A, Henry T, Margolis JJ, Chan K, Monack DM.** 2007. In vivo negative selection screen identifies genes required for Francisella virulence. Proc. Natl. Acad. Sci. U. S. A. **104**:6037–6042.
8. **Metzger DW, Bakshi CS, Kirimanjeswara G.** 2007. Mucosal immunopathogenesis of Francisella tularensis. Ann. N. Y. Acad. Sci. **1105**:266–283.
9. **Conlan JW, Chen W, Shen H, Webb A, KuoLee R.** 2003. Experimental tularemia in mice challenged by aerosol or intradermally with virulent strains of Francisella tularensis: bacteriologic and histopathologic studies. Microb. Pathog. **34**:239–248.
10. **Hall JD, Woolard MD, Gunn BM, Craven RR, Taft-Benz S, Frelinger JA, Kawula TH.** 2008. Infected-host-cell repertoire and cellular response in the lung following inhalation of Francisella tularensis Schu S4, LVS, or U112. Infect. Immun. **76**:5843–5852.
11. **Bosio CM, Dow SW.** 2005. Francisella tularensis induces aberrant activation of pulmonary dendritic cells. J. Immunol. **175**:6792–6801.
12. **Hajjar AM, Harvey MD, Shaffer SA, Goodlett DR, Sjostedt A, Edebro H, Forsman M, Bystrom M, Pelletier M, Wilson CB, Miller SI, Skerrett SJ, Ernst RK.** 2006. Lack of in vitro and in vivo recognition of Francisella tularensis subspecies lipopolysaccharide by Toll-like receptors. Infect. Immun. **74**:6730–6738.
13. **Bosio CM, Bielefeldt-Ohmann H, Belisle JT.** 2007. Active suppression of the pulmonary immune response by Francisella tularensis Schu4. J. Immunol. **178**:4538–4547.
14. **Chong A, Celli J.** 2010. The Francisella intracellular life cycle: toward molecular mechanisms of intracellular survival and proliferation. Front. Microbiol. **1**:138. doi:10.3389/fmicb.2010.00138.
15. **Yee D, Rhinehart-Jones TR, Elkins KL.** 1996. Loss of either CD4+ or CD8+ T cells does not affect the magnitude of protective immunity to an intracellular pathogen, Francisella tularensis strain LVS. J. Immunol. **157**:5042–5048.
16. **Collazo CM, Sher A, Meierovics AI, Elkins KL.** 2006. Myeloid differentiation factor-88 (MyD88) is essential for control of primary in vivo Francisella tularensis LVS infection, but not for control of intra-macrophage bacterial replication. Microbes Infect. **8**:779–790.
17. **Leiby DA, Fortier AH, Crawford RM, Schreiber RD, Nacy CA.** 1992. In vivo modulation of the murine immune response to Francisella tularensis LVS by administration of anticytokine antibodies. Infect. Immun. **60**:84–89.
18. **Anthony LS, Ghadirian E, Nestel FP, Kongshavn PA.** 1989. The requirement for gamma interferon in resistance of mice to experimental tularemia. Microb. Pathog. **7**:421–428.
19. **Woolard MD, Hensley LL, Kawula TH, Frelinger JA.** 2008. Respiratory Francisella tularensis live vaccine strain infection induces Th17 cells and prostaglandin E2, which inhibits generation of gamma interferon-positive T cells. Infect. Immun. **76**:2651–2659.
20. **Lin Y, Ritchea S, Logar A, Slight S, Messmer M, Rangel-Moreno J, Guglani L, Alcorn JF, Strawbridge H, Park SM, Onishi R, Nyugen N, Walter MJ, Pociask D, Randall TD, Gaffen SL, Iwakura Y, Kolls JK, Khader SA.** 2009. Interleukin-17 is required for T helper 1 cell immunity and host resistance to the intracellular pathogen Francisella tularensis. Immunity **31**:799–810.
21. **Markel G, Bar-Haim E, Zahavy E, Cohen H, Cohen O, Shafferman A, Velan B.** 2010. The involvement of IL-17A in the murine response to sub-lethal inhalational infection with Francisella tularensis. PLoS One **5**:e11176. doi:10.1371/journal.pone.0011176.
22. **Nano FE, Zhang N, Cowley SC, Klose KE, Cheung KK, Roberts MJ, Ludu JS, Letendre GW, Meierovics AI, Stephens G, Elkins KL.** 2004. A Francisella tularensis pathogenicity island required for intramacrophage growth. J. Bacteriol. **186**:6430–6436.
23. **Meibom KL, Dubail I, Dupuis M, Barel M, Lenco J, Stulik J, Golovliov I, Sjostedt A, Charbit A.** 2008. The heat-shock protein ClpB of Francisella

tularensis is involved in stress tolerance and is required for multiplication in target organs of infected mice. Mol. Microbiol. **67**:1384–1401.
24. **Conlan JW, Shen H, Golovliov I, Zingmark C, Oyston PC, Chen W, House RV, Sjostedt A.** 2010. Differential ability of novel attenuated targeted deletion mutants of Francisella tularensis subspecies tularensis strain SCHU S4 to protect mice against aerosol challenge with virulent bacteria: effects of host background and route of immunization. Vaccine **28**:1824–1831.
25. **Twine S, Shen H, Harris G, Chen W, Sjostedt A, Ryden P, Conlan W.** 2012. BALB/c mice, but not C57BL/6 mice immunized with a DeltaclpB mutant of Francisella tularensis subspecies tularensis are protected against respiratory challenge with wild-type bacteria: association of protection with post-vaccination and post-challenge immune responses. Vaccine **30**: 3634–3645.
26. **Chamberlain RE.** 1965. Evaluation of live tularemia vaccine prepared in a chemically defined medium. Appl. Microbiol. **13**:232–235.
27. **LoVullo ED, Molins-Schneekloth CR, Schweizer HP, Pavelka MS, Jr.** 2009. Single-copy chromosomal integration systems for Francisella tularensis. Microbiology **155**:1152–1163.
28. **Woolard MD, Wilson JE, Hensley LL, Jania LA, Kawula TH, Drake JR, Frelinger JA.** 2007. Francisella tularensis-infected macrophages release prostaglandin E2 that blocks T cell proliferation and promotes a Th2-like response. J. Immunol. **178**:2065–2074.
29. **Porter BB, Harty JT.** 2006. The onset of CD8+-T-cell contraction is influenced by the peak of Listeria monocytogenes infection and antigen display. Infect. Immun. **74**:1528–1536.
30. **Williams MA, Bevan MJ.** 2004. Shortening the infectious period does not alter expansion of CD8 T cells but diminishes their capacity to differentiate into memory cells. J. Immunol. **173**:6694–6702.
31. **Wong P, Pamer EG.** 2001. Cutting edge: antigen-independent CD8 T cell proliferation. J. Immunol. **166**:5864–5868.
32. **Broms JE, Meyer L, Lavander M, Larsson P, Sjostedt A.** 2012. DotU and VgrG, core components of type VI secretion systems, are essential for Francisella LVS pathogenicity. PLoS One **7**:e34639. doi:10.1371/journal.pone.0034639.
33. **Chen W, Shen H, Webb A, KuoLee R, Conlan JW.** 2003. Tularemia in BALB/c and C57BL/6 mice vaccinated with Francisella tularensis LVS and challenged intradermally, or by aerosol with virulent isolates of the pathogen: protection varies depending on pathogen virulence, route of exposure, and host genetic background. Vaccine **21**:3690–3700.
34. **Schmitt DM, O'Dee DM, Horzempa J, Carlson PE, Jr, Russo BC, Bales JM, Brown MJ, Nau GJ.** 2012. A Francisella tularensis live vaccine strain that improves stimulation of antigen-presenting cells does not enhance vaccine efficacy. PLoS One **7**:e31172. doi:10.1371/journal.pone.0031172.
35. **Woolard MD, Barrigan LM, Fuller JR, Buntzman AS, Bryan J, Manoil C, Kawula TH, Frelinger JA.** 2013. Identification of *Francisella novicida* mutants that fail to induce prostaglandin E_2 synthesis by infected macrophages. Front. Microbiol. **4**:16. doi:10.3389/fmicb.2013.00016.
36. **Maier TM, Pechous R, Casey M, Zahrt TC, Frank DW.** 2006. In vivo Himar1-based transposon mutagenesis of Francisella tularensis. Appl. Environ. Microbiol. **72**:1878–1885.
37. **Gray CG, Cowley SC, Cheung KK, Nano FE.** 2002. The identification of five genetic loci of Francisella novicida associated with intracellular growth. FEMS Microbiol. Lett. **215**:53–56.
38. **Tempel R, Lai XH, Crosa L, Kozlowicz B, Heffron F.** 2006. Attenuated Francisella novicida transposon mutants protect mice against wild-type challenge. Infect. Immun. **74**:5095–5105.
39. **Kalinski P, Vieira PL, Schuitemaker JH, de Jong EC, Kapsenberg ML.** 2001. Prostaglandin E(2) is a selective inducer of interleukin-12 p40 (IL-12p40) production and an inhibitor of bioactive IL-12p70 heterodimer. Blood **97**:3466–3469.
40. **Schnurr M, Toy T, Shin A, Wagner M, Cebon J, Maraskovsky E.** 2005. Extracellular nucleotide signaling by P2 receptors inhibits IL-12 and enhances IL-23 expression in human dendritic cells: a novel role for the cAMP pathway. Blood **105**:1582–1589.
41. **Sheibanie AF, Tadmori I, Jing H, Vassiliou E, Ganea D.** 2004. Prostaglandin E2 induces IL-23 production in bone marrow-derived dendritic cells. FASEB J. **18**:1318–1320.
42. **Hunter CA.** 2005. New IL-12-family members: IL-23 and IL-27, cytokines with divergent functions. Nat. Rev. Immunol. **5**:521–531.
43. **Zolkiewski M.** 2006. A camel passes through the eye of a needle: protein unfolding activity of Clp ATPases. Mol. Microbiol. **61**:1094–1100.
44. **Chastanet A, Derre I, Nair S, Msadek T.** 2004. clpB, a novel member of the Listeria monocytogenes CtsR regulon, is involved in virulence but not in general stress tolerance. J. Bacteriol. **186**:1165–1174.
45. **Lourdault K, Cerqueira GM, Wunder EA, Jr, Picardeau M.** 2011. Inactivation of clpB in the pathogen Leptospira interrogans reduces virulence and resistance to stress conditions. Infect. Immun. **79**:3711–3717.
46. **Capestany CA, Tribble GD, Maeda K, Demuth DR, Lamont RJ.** 2008. Role of the Clp system in stress tolerance, biofilm formation, and intracellular invasion in Porphyromonas gingivalis. J. Bacteriol. **190**:1436–1446.
47. **Kannan TR, Musatovova O, Gowda P, Baseman JB.** 2008. Characterization of a unique ClpB protein of Mycoplasma pneumoniae and its impact on growth. Infect. Immun. **76**:5082–5092.
48. **Turner AK, Lovell MA, Hulme SD, Zhang-Barber L, Barrow PA.** 1998. Identification of Salmonella typhimurium genes required for colonization of the chicken alimentary tract and for virulence in newly hatched chicks. Infect. Immun. **66**:2099–2106.